ABSTRACT

CHARACTERIZATION OF ELECTROSPUN DLPLGA NANOFIBERS FOR A DRUG DELIVERY SYSTEM FOR INTRACRANIAL TUMORS AND AVMs

by
Kimberly A. Griswold

Electrospinning processes apply electric fields to a polymer solution in order to produce strands of polymer in the nanoscale range. These polymer fibers are manipulated for their porosity, high surface area, fineness and uniformity. In order to create the ideal drug delivery system for intracranial arteriovenous malformations (AVMs) and tumors, D, L poly-(lactice-poly-glycolide) (DLPLGA) nanofibers were electrospun in a tetrahydrofuran (THF) solvent. Three different concentration ratios of DLPLGA, 85/15, 80/20, and 75/25 were analyzed to obtain the prime base for drug annexation. 1,3-bis (2-chloroethyl)-1-nitrosourea (BCNU) was then codissolved with the DLPLGA nanofibers to form a homogenous solution, electrospun, and analyzed for drug characterization.

The SEM analysis showed that fiber diameter is not a function of drug presence. The TGA graphs showed little variation in mass loss in comparing the electrospun fiber to the drug combined fiber. The DSC analysis provided a Tg value around 48-53°C for both the raw polymer and the electrospun fiber. This provided proof that the electrospinning process does not affect the chemical nature of the polymer. The presence of BCNU on the polymer (chose 80/20-10wt%) was determined by the change in Tg observed on the DSC graphs from a value of 48-53°C to two values of 12.69°C and 18.94°C.

CHARACTERIZATION OF ELECTROSPUN DLPLGA NANOFIBERS FOR A DRUG DELIVERY SYSTEM FOR INTRACRANIAL TUMORS AND AVMs

by
Kimberly A. Griswold

A Thesis
Submitted to the Faculty of
New Jersey Institute of Technology
In Partial Fulfillment of the Requirements for the Degree of
Master of Science in Biomedical Engineering

Department of Biomedical Engineering

January 2004

Blank Page

APPROVAL PAGE

CHARACTERIZATION OF ELECTROSPUN DLPLGA NANOFIBERS FOR A DRUG DELIVERY SYSTEM FOR INTRACRANIAL TUMORS AND AVMs

Kimberly A. Griswold

Dr. Michael Jaffe, Thesis Advisor — Date
Research Professor of Biomaterials, NJIT

Dr. Charles J. Prestigiacomo, Thesis Co-Advisor — Date
Medical Doctor and Assistant Professor of Neurological Surgery and Radiology, UMDNJ

Dr. Michael Huang, Committee Member — Date
Associate Professor of Chemical Engineering, NJIT

Dr. Treena Arinzeh, Committee Member — Date
Assistant Professor of Biomedical Engineering, NJIT

BIOGRAPHICAL SKETCH

Author: Kimberly Ann Griswold

Degree: Master's of Science

Date: January 2004

Undergraduate and Graduate Education:

- Master of Science in Biomedical Engineering
  Concentration in Polymer Science and Biomaterials,
  New Jersey Institute of Technology, Newark, NJ, 2004

- Bachelor of Science in Biomedical Engineering
  Concentration in Optics,
  University of Rochester, Rochester, NY, 2002

Major: Biomedical Engineering
Concentration in Polymer Science and Biomaterials

Dedicated to the memory of my grandfather, Augustus W. Griswold, co-founder of Dynak Incorporated, engineer, innovative thinker, and inventor. Also to my devout and patient family and friends who through enlightenment allowed me to be comfortable in my own skin. Finally, to my Korean family, all inclusive, known and unknown - for the gift of life, new and old, and for anonymity.

ACKNOWLEDGMENT

I would first like to recognize the support and guidance of Dr. Michael Jaffe and Dr. Charles J. Prestigiacomo in not only my academic endeavors, but my personal ones as well. Dr. Michael Jaffe served as my research advisor, but was very influential in the academic path chosen and the career choices I have made. Dr. Charles J. Prestigiacomo served as my assistant research advisor and provided constant support, encouragement, and intellectual stimulation to keep me motivated throughout the project.

Special Thanks goes to Dr. Michael Huang for providing such an amazing academic experience and guiding me to a particular field of concentration for this thesis research. It is he to whom I owe all my newfound interest and my desire to obtain greater knowledge in polymer science.

Appreciation to my fellow graduate students in the Medical Device and Concept Laboratory, particularly Shobana Shanmugasundaram for her assistance and knowledge in the electrospinning process, and fine-tuned SEM and computer technique. Finally, particular acknowledgment to Joseph Pickton for his judgment and knowledge of Polymer Science, his support and strong shoulder to lean on, and his keen wit for humor.

TABLE OF CONTENTS

TABLE OF CONTENTS
(Continued)

Chapter **Page**

LIST OF TABLES

LIST OF FIGURES

LIST OF FIGURES
(Continued)

LIST OF FIGURES
(Continued)

CHAPTER 1

INTRODUCTION

1.1 Objective

The objective for this thesis research is to use the electrospinning process in order to create a D, L poly-(lactide-poly-glycolide) (DLPLGA) drug delivery system, using the drug 1,3-bis (2-chloroethyl)-1-nitrosourea (BCNU), to target intracranial vascular malformations and tumors. By creating such a system to the nanoscale, delivery of the system can be done by a guided catheter (endovascular techniques) and decreases the invasiveness of the treatment procedure in comparison to current practice regimens.

By using the electrospinning technique, a non-woven sheet of nanofibers is created by which porosity, surface area, fineness, uniformity of fiber diameter, and pattern thickness of the sheet can be manipulated. The chemotherapeutic agent, BCNU, is known to alkylate the DNA of tumor cells causing apoptosis. To conduct the research, DLPLGA, a widely used polymer for drug release with well-characterized degradation properties in concentration ratios of 85/15 (high inherent viscosity [IV], GMP), 80/20 (high IV, not GMP), and 75/25 (high IV, GMP) was used. All three ratios were tested in order to obtain the ideal method for drug delivery. Each of the ratios had different degradation rates (different release profiles), therefore met different standards for the system.

In order to define the ideal system, the electrospinning process allows for DLPLGA nanoscale fibers to be conjoined with BCNU and deliver the drug through a steady degradation rate over a targeted period of time. The release rate of the drug is dependent upon the degradation rate, which is based upon the characteristics of the

polymer. By doing so, it is anticipated that the drug would be packaged in its most stable state and concentrated form for immediate release. The solvent, Tetrahydrofuran (THF), would allow for the insertion of the delivery of this system through a guided catheter, performed by an endovascular surgeon. The drug would be released by oxidation (by means of hydrolysis) of the nanopolymer fibers at target site, thus providing high concentrations of drug to the tumor bed while potentially greatly limiting any systemic side effects.

The research done in this thesis is an initial step in creating a more complex drug delivery system. An electrospun sheet will most certainly not be the final physical form for the delivery, but it is sufficient for the initial characterization of the system for proof of concept.

1.2 Background Information

It is essential to identify the problem and create a solution that has the ability to have variance in drug choice and material choice. In neuroscience, in choosing AVM's and intracranial tumors as the problem, an extensive variety of uses for the drug delivery system were available. The use of BCNU as the drug of choice was to narrow down a focal point for the drug delivery system model. With BCNU to create and test the model system, it could then also be determined if other drugs could be used in place of the BCNU with a set of data for comparison. The sheet formation used in this model is not the ideal morphology, but is compatible for the initial stages of the research. Other electrospun polymer morphology is plausible and should be investigated.

1.2.1 Intracranial Central Nervous System Disease

Arteriovenous Malformations (AVMs) are an abnormal collection of blood vessels that affect approximately 250,000 people (one out of 1000 people are born with an AVM) in the United States [7]. Histologically, these are lesions (also known as an AVM nidus) that (typically located as a connection between the artery and the vein) provide nutrient and gas exchange to the tissue. The resultant low-resistance, high pressure and high flow state within the nidus creates a shunt. Thus, in an AVM, blood flows from arteries straight through the shunt and into the venous system [6]. Consequently, much of the blood can be diverted from the surrounding tissue in order to flow through the AVM, since the AVM provides less resistance to blood flow than the capillary network. Increased blood flow through the AVM increases the pressure on the vessels, which can result in formation of aneurysms and possible hemorrhage (2- 4% chance of bursting per year) [Figure 1.1] [7]. In short description, 1 point is given to a small tumor, the size of approximately 3cm or an eloquent or deep AVM. Non-eloquent and superficial AVM's are given zero points. Medium size AVM's are approximately 3-6cm with a value of two points and large size AVM's in reference to greater than 6cms with a value of three points.

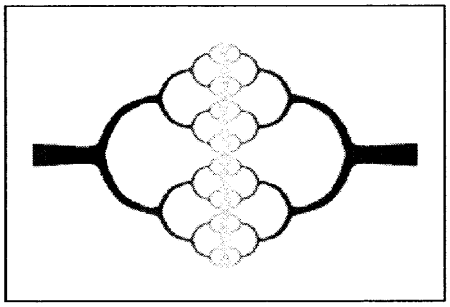

(a)

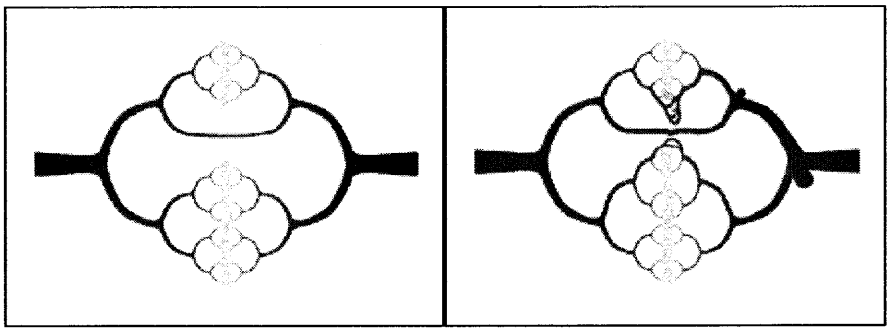

(b) (c)

Figure 1.1 (a) Normal arteriovenous formation, (b) AVM, (c) advanced AVM with down stream aneurysm.

Cerebral AVMs represent about 80% of all intracranial vascular malformations. Exact pathogenesis is not known though a male preponderance is reported by almost all studies [8]. Incidence of bleeding is about 70% over course of lifetime [8], and is unrelated to stress, trauma, and hypertension. There exist some studies that show the possibility of rupture during the onset of pregnancy (questionable). However, in general, the risk of bleeding is greater in children, but risk percentages decline after the age of 40 [8]. There is some evidence to suggest that because of specific hemodynamic reasons, small AVMs have a higher chance of rupture due to the build up of higher pressure in the feeding artery.

In addition to hemorrhage, seizures are a common presentation of AVMs occurring in about 30% of all cases and are associated with subclinical development in about 7% of cases with the average age of onset of 25years [8]. Malformations are so complex, because they can affect individuals during the most productive years of their lives with such devastating consequences, and because current treatment carries substantial risk, developing a system, which can safely and effectively treat these lesions is vital. A drug delivery system that is compatible to all and accessible to all areas is favored.

Primary malignant tumors of the central nervous system, despite years of study, still carry a mean life expectancy of 13 years. There exists a four-tier system for assessing tumor activity and progression (as per the world health organization [WHO]): Grade 4 being rapidly growing and malignant and 1 being the slowest. The area of the brain and the size of the tumor are factors involved in determining the grade level. For the lowest grade, grade 1, treatment can be as simple as surgery. However, for higher-grade tumors, the solution is not as simple due to the invasion of cancerous cells into surrounding tissue, which may even be transported by spinal fluid to completely different regions of the brain, and spinal region.

Each of the grade levels applies to each type of tumor, with slight variations in description based on the cell characteristics and treatment methods. Astrocytomas are tumors formed from astrocyte cells, which form part of the brain's supportive (neuroglial) tissue [9]. Grade 2 has a 34% 5 year survival rate without treatment. With radiation therapy, survival increases to about 70%. With grade 3, the average survival of patients is 18months, with diagnosis by surgery or stereotactic biopsy and follow-up with

radiation therapy and chemotherapy [9]. In grade 4 patients, the average (mean) survival after diagnosis without treatment is 17weeks. Survival is extended up to 30weeks with biopsy followed by radiation therapy and 37weeks with surgical removal of most of the tumor tissue combined with radiation therapy. The best treatment involves stereotactic volumetric resection of the tumor tissue component followed by radiation therapy, for a patient longevity of approximately 51weeks. Glioblastoma Multiforme (grade 4 astrocytoma) makes up 25% of all primary brain tumors. This tumor is able to infiltrate throughout the entire brain and is marked by areas of necrosis (dead tumor cells) [9].

Metastatic tumors are caused by cells from other tumors in the body transported through the blood stream to the brain. The brain tissue around the tumor begins to swell (edema), causing focal neurological deficits, lethargy, and in extreme cases coma and death. Oligodendrogliomas originate from oligodendroglial cells that form myelin, the fatty substance that surrounds the axons of nerve cells and provides the insulation, which makes nerve cell electrical transmission faster and more efficient [9]. Tumor growth depends on the rate of mitosis and rate of apoptosis. When the mitotic rate of the oligodendroglial cells has exceeded the mitotic rate of the other cells, therefore becoming the dominant cell type, the degree of classification time changes from 6months to 30 years [9]. Most glial tumors have two growth patterns: solid tumor tissue and infiltrating tumor cells, which are judged by progressive enlargement on a computerized tomography (CT) or magnetic resonance imaging (MRI). Solid tumor tissue is characterized by the increase in mass from the production of new blood vessels from those that supply the brain with oxygen, glucose and other nutrients. The new blood vessels function to supply the growing tumor cells with oxygen, glucose and other nutrients, directly infiltrating the

source of nutrients that should supply the brain. Low grade (low blood supply needed) tumors may not be apparent on a CT or MRI due to lack of contrast enhancement (anaplastic or malignant require large blood supply) and may be removed without neurological deficit (solid tumor tissue either displaces or replaces brain substance) depending on the lesion's location [9].

Isolated tumor cells can move between the fibers of the brain, with the entire tumor consisting of these cells which reside in "sick" but still functioning brain tissue, which makes removal difficult [9]. Most low-grade infiltrating tumor cells are visible as a hypodensity on a CT and increased T1 and T2 signal on an MRI because the tumor cells tend to draw water into the infiltrated brain tissue [9]. If isolated tumor cells are not great enough in number to change the local osmolality and thus increase the amount of water surrounding them, the CT and MRI will show no changes and appear normal in the area [9]. If some tumor cells still reside in the tissue after treatment, it is guaranteed that the tumor will return. These types of tumors are more frequent in young and middle-aged adults.

1.2.2 Current Treatment Methods

To locate problematic areas, computerized tomography (CT's), magnetic resonance imaging (MRI's), and Angiogramss (x-ray movies of the blood flowing through the blood vessels, made by injecting contrast into the arteries going into the head and taking a series of x-ray films) are used. However, not all of these methods are completely accurate. As mentioned in section 1.2.1 Intracranial Central Nervous System Disease, there are a variety of lesions whose behavior is not always predictable or traceable. If the cells do

not produce enough of a difference in osmolality compared to normal conditions, a CT or MRI may not detect the malformation.

Embolization is a method of plugging the blood vessels of the AVM, by an x-ray guided catheter from the femoral artery in the leg up into the area to be treated [6]. The AVM's feeder vessels are then sealed off from within using an epoxy applied by an angiographic catheter [7]. Embolization is usually done in preparation for surgery to reduce the blood flow within the AVM or is combined with radiation therapy to obliterate the AVM. The benefits of this method are that: (1) it does not require a craniotomy; (2) eloquent deep areas can be treated by doing small areas at a time and allowing the surrounding brain to recover; and (3) testing of the importance of the area can be done by injection of medication into the area before permanent treatment is done [6]. However, it requires multiple treatments, multiple entries into the brain, the use of new materials under "Investigation" (not yet approved by the FDA or not GMP regulated), and is used as an adjunct to another method (often combined with surgery or radiosurgery) [6].

Radiation therapy is a noninvasive procedure that uses ionizing radiation to damage the DNA in all cells (normal cells can repair damage but tumor cells cannot). Irradiated tissue temporarily swells, that there exists a maximum volume above which the amount of swelling can cause damage. Therefore to minimize the dose given, the radiation beam is directed from several angles toward the site by a linear accelerator. The efficacy of radiation treatment is limited by the size of the lesion, with the limit at no greater than 3cm due to drastic reduction in cure rate, with a concomitant increase in complication rate. There are different techniques being developed for radiation therapy. Stereotactic Brachytherapy is an invasive method that uses multiple sources placed

within tumor tissue to provide a dose field, with 40% of patients requiring an operation afterwards [9]. Boron Neutron Capture Therapy (BNCT) uses the theories of atomic physics in which a boron compound is taken up by tumor cells, neutrons are absorbed into the Boron, forming gamma irradiation and an alpha particle which kills the tumor cell [9]. This method is usually used for tumors and not AVMs.

Surgery is an invasive procedure that involves the excision of some or the entire lesion, with preservation of normal brain tissue. There are three steps to the procedure: (1) establish tumor cell type and grade, (2) relieve internal pressure, and (3) reduce the tumor burden. A craniotomy is where a portion of the skull is temporarily removed, allowing the surgeon access to the lesion. Stereotactic procedures precisely localize areas inside the head for biopsy, such that a stereotactic biopsy (probe directed by stereotactic frame to tumor) is performed. Another similar method, the computer-assisted volumetric stereotaxis gathers, stores and reformats imaging-derived, 3-D volumetric information defining an intracranial lesion with respect to the surgical field in order to plan and simulate the surgical procedure beforehand [9]. Volumetric stereotaxis can minimize the incision and subsequent injury to brain tissue, thus maximizing tumor removal and reducing postoperative complications and neurological morbidity [9]. Stereotactic radiosurgery claims a success rate of 80% after two years of follow-up, depending on the histologic grade of the lesion [8]. As efficient as all these methods are, surgery still is an invasive process that involves the risk of bleeding and infection, a long recuperation time, and is dependent on how accessible (how deep into the brain tissue) the lesion is.

Chemotherapy proves to be a promising area for advancement in approaching the problem from a different perspective. Most agents are incorporated into and alkylate the

DNA of rapidly dividing tumor cells like BCNU, PCNU, Procarbazine and Carboplatin. Vincristine poisons the mitotic process and VP-16 (Etoposide is a semisynthetic derivative of podophyllotoxin used in the treatment of certain neoplastic diseases) incorporated in tumor cell wall proteins inhibits the production of microtubules. Topotecan enhances the effect of radiation therapy by intravenously affecting rapidly dividing tumor cells and normal cells from bone marrow and bowel. Most of these agents may result in the reduction of white blood cells (causing severe, potentially life-threatening infections), red blood cells (causing anemia), and platelets (thrombocytopenia - resulting in blood clotting disorders and bleeding). However they are the only agents that can overcome the problems with glial primary brain tumors. Many tumor cells infiltrate surrounding brain tissue where the blood-brain barrier (which excludes large molecules) is intact. These agents can reach cells in the major mass of the tumor, which is supported by leaky tumor blood vessels, via these blood vessels. The blood-brain barrier protects tumor cells residing within intact brain tissue surrounding the tumor, but can be disrupted medically by chemotherapy.

Guilford pharmaceuticals markets polyanhydride Gliadel wafers for treating a type of brain cancer called glioblastoma multiforme. Wafers consist of new polymers impregnated with carmustine (BCNU), a toxic antitumor medication and are implanted at the tumor site, release the drug locally where it is needed while reducing systemic side effects such as liver or kidney damage. However, the wafer does have other side affects due to the drug delivery system and the means of implantation. In clinical trials, 19% of patients reported new or worsened seizure symptoms and 14% experienced healing abnormalities (such as cerebral fluid leaks, subdural fluid collections, wound

breakdown). Other adverse reactions included intracranial infections, pain in back and chest, hypertension, diarrhea, fever, rashes, and urinary tract infections. Combination of treatments is the best method in curing brain tumors and AVMs. They can be tailored to the specific AVM type or tumor type and patient considerations, but requires additional steps, time and coordination [6].

1.2.3 Pharmacokinetics of BCNU

BCNU, [1,3-bis (2-chloroethyl)-1-nitrosourea] also known as carmustine has the structural formula found in Figure 1.2.

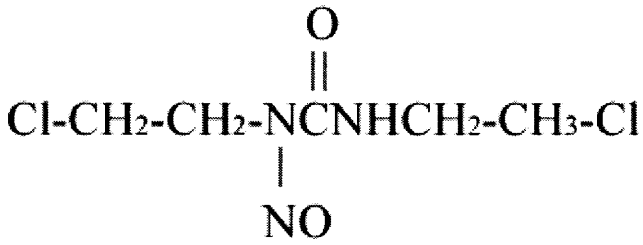

Figure 1.2 [1,3-bis (2-chloroethyl)-1-nitrosourea].

The chemical activity of BCNU is to alkylate the DNA and RNA of cells. It has been known to degrade both spontaneously and metabolically the DNA cross-links hypothesized to derive from chloroethyl carbonium ion [22]. Based on intravenous studies, the average terminal half-life (based on dosage range from 30 to 170 mg/m^2) was 22minutes, with a clearance of 56 ml/min/kg, and a steady-state volume of distribution of 3.25 L/kg [22]. In a 200mg/m^2 intravenous dosage, 60-70% was excreted through urine and 6-10% expired as carbon dioxide over a 96 hour time span.

The remaining 20-30% has not been accounted for yet. The degradation rate occurs at such a high rate, that within 15minutes of injection, no intact drug is detectable. Studies have shown that the reactive nature of the drug is so extensive that it can be carried by cerebral blood flow or cerebrospinal fluid flow and overcome the blood-brain barrier with in the confines of brain tissue a distance away from the implantation site of the device.

The blood-brain barrier is overcome because of the compound's high lipid solubility and the relative lack of ionization at physiological pH. Due to its toxic nature, BCNU may also inhibit several key enzymatic processes by carbamoylation of amino acids in proteins. Long-term usage of a nitrosoureas product is associated with development of secondary malignancies. It has also been shown to be embryotoxic in rats and rabbits and if injected in an intraarterial intracarotid route, associated with ocular toxicity. In a study done on male rats given the dosage allotted for humans, fertility was impaired and carcinogenic and mutagenic effects were noted. Intravenously administered, many other side affects are concurrent upon delivery. These are pulmonary toxicity (such as fibrosis), gastrointestinal toxicity, hepatoxicity, nephrotoxicity, and skin hyperpigmentation upon contact.

The dry form of the active agent can be stable for up to two years in temperature of 2°C - 8°C (36°F - 46°F) and when suspended in diluent, eight hours at room temperature, away from sunlight. It has a low melting point at 30.5°C to 32°C (86.9°F - 89.6°F) and can effortlessly liquefy (from dry form) when temperatures change.

1.2.4 Biodegradable Polymers

The first FDA-cleared PLGA product was the Lupron Depot drug-delivery system (TAP Pharmaceutical Products Inc.; Lake Forest, IL), a controlled release device for the treatment of advanced prostate cancer that used biodegradable microspheres of 75:25 lactide/glycolide to administer leuprolide acetate over periods as long as four months (replacing daily injections) [13]. "Another drug-delivery device, the Gliadel Wafer (Guilford Pharmaceuticals Inc.; Baltimore, MD), is used to prolong the life of patients suffering from a particularly deadly form of brain cancer, glioblastoma multiforme. In this case, dime sized wafers of a biodegradable polyanhydride copolymer-poly [bis (p-carboxyphenoxy) propane: sebacic acid] in a 20:80 molar ratio - are implanted directly into the brain to deliver a powerful chemotherapeutic agent (BCNU) that has deleterious side affects when administered systemically [13]. Release of the drug delivery in the implantable wafers was stimulated by the presence of poly (N-vinylpyrrolidone) (PVP) or sodium chloride (NaCl).

However, using different biomaterials raises considerations on biocompatibility, the reaction of the patient to the material, the effectiveness of the drug delivery system, and the cost [Appendix B]. For the purpose of this research, the amorphous form of Polyglycolic acid/Polylactic acid copolymer (PGLA or PLAGA) (some ratio of it discussed later) was chosen for the base material. This biodegradable synthetic polymer is amorphous with a weight of 40-100kD. It has a decomposition of 100% in 60-90 days (observed in rat stem cells). A biodegradable polymer is optimal for drug delivery systems by controlled processing so that optimal release of kinetics of the drug or active agent is achieved. Polymer degradation is accelerated by greater hydrophilicity in the

backbone or end groups, greater reactivity among hydrolytic groups in the backbone, less crystallinity, greater porosity, and smaller finished device size [13].

When considering a biodegradable polymer, one has to think about the physiologic effects the mechanical or chemical process and their products may have on the surrounding area. In a study done in Atlanta Georgia in 2002, polymer degradation affected cell growth. The data showed that direct addition of either glycolic or lactic acids to control cell cultures without PLAGA resulted in proportional cytotoxicity [10]. The metabolic breakdown products from PLAGA significantly lowered the pH of the environment and that sustained cell viability on PLAGA membrane is partially dependent on the local pH, especially in controlled limited *in vitro* cultures [10].

This possibly is beneficial since the goal is to deter cell growth. Still, caution must be used in preventing damage to viable non-cancerous cells. In addition, the flow of the blood should flush the residual components out of the system. The pH is probably not an issue due to the extreme buffering capacity of blood, which will continually wash away any released products from the degradation of the PLGA polymer. The pH difference may only be a concern when dealing with the drug delivery, the actual drug performance, and any conditions the patient may have that may be affected by the pH change.

PGLA is comprised of PLA and PGA in respective ratios. Both contribute to the mechanical toughness and strength found in either the crystalline or the semicrystalline form used for biological application [Appendix A]. Polymers have very low polydisperity index ratios (PDI) that characterize the maintenance of the mechanical and structural strength [14].

All the polymers have very low polydisperity index ratios (P.D.I). For example, the P.D.I. ratio for PLA is around 1.6-1.9, in order to maintain mechanical and structural consistency. Utilizing ring-opening polymerization combines the most common method of commercial production of PLA and PGA with an insertion mechanism using a metal oxide4 [14]. A more amorphous form of the polymer can be used for drug delivery devices while the crystalline form is good for building scaffolding and other biodegradable structures. PLGA, for example is completely amorphous so therefore it is used only in drug delivery devices. The use of certain drugs, for example, is prohibited by the relatively high temperatures used in constructing these polymers. Another drawback is in the controlled release of drugs. Bulk erosion has a somewhat inconsistent release of drug. Depending on the amount of drug loaded onto the polymer, its hydrophilic or hydrophobic properties, the initial rate of release can vary [14].

1.2.5 Kinetics of Drug Release

Controlled drug delivery is directly dependent upon the nature of the biodegradable polymer (if degradation is the control of release rate). The factors that affect release rate are chemical structure, chemical composition, processing conditions, morphology, and site of implantation. Chemical structure includes molecular-weight distribution, shape, and physical factors (shape and size changes, variations of diffusion coefficients, mechanical stresses, stress- and solvent-induced cracking). Chemical composition involves the presence of ionic groups, molecular weight, the presence of low-molecular-weight compounds, adsorbed and absorbed compounds (water, lipids, ions), physicochemical factors (ion exchange, ionic strength, pH), and mechanism of hydrolysis

(enzymes versus water) [20]. Processing conditions with storage history, sterilization processes, and annealing have an affect on the final overall functionality of the release system. Distribution of repeat units in multimers, the presence of unexpected units or chain defects, and configuration structure all fall under the category of morphology (amorphous/semicrystalline, microstructures, residual stresses) [20].

The release of the active agent may be constant over a long period, it may be cyclic over a long period, or the environment or other external events may trigger it in order to maintain the correct amount of dosage (preventing over- and underdosing) [20]. There are three primary mechanisms of drug release:

(1) diffusion; (2) degradation; (3) swelling followed by diffusion. In some drug delivery systems, a combination of the mechanisms was used. Diffusion can occur on a macroscopic scale, as through pores in the polymer matrix, or on a molecular level, by passing between polymer chains, where in both cases the morphology of the polymer is the controlled-release device [20]. Diffusion also can occur when the drug passes from the polymer matrix (homogenous system formed from the union of polymer and active agent) into the external environment. As the release continues, its rate normally decreases with this type of system, since the active agent has a progressively longer distance to travel and therefore requires a longer diffusion time to release [20].

Reservoir systems are designed to use the method of diffusion by enclosing an active agent (solid drug, dilute solution, or highly concentrated drug solution with polymer matrix) with a material that acts as a membrane, facilitating exiting or entering molecules at a consistent rate. For the reservoir systems shown in Figures 1a and 1b, the drug delivery rate can remain fairly constant [20]. The membrane of the reservoir can

have a uniform polymer coating on either one side of both sides, depending on what the stimulus for the active agent is. The system shown in Figure 1.3(a) is representative of an implantable or oral reservoir delivery system, whereas the system shown in Figure 1.3(b) illustrates a transdermal drug delivery system, in which only one side of the device will actually be delivering the drug [20].

The environment the active agent is released in can regulate control of the drug delivery. Once the active agent has been released into the external environment, an additional series of diffusional and active transport steps can occur that have a direct relationship with environmental factors.

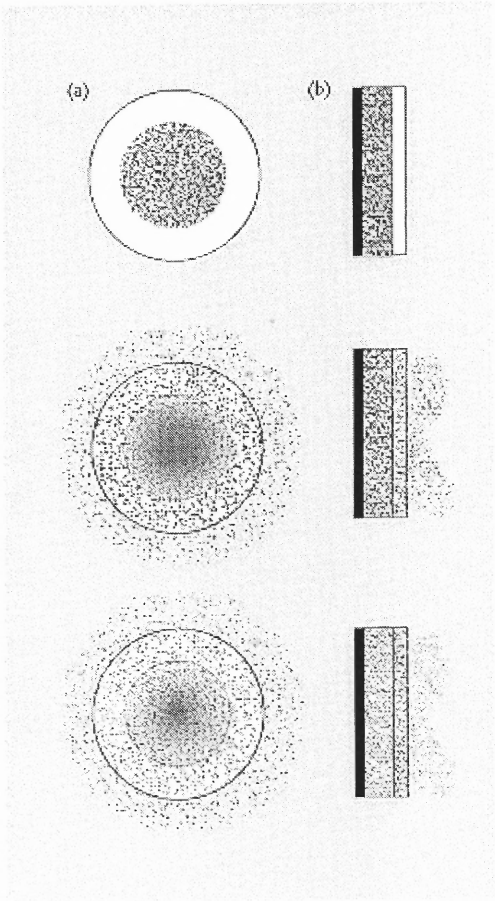

Figure 1.3 Reservoir systems (a) implantable/oral, (b) transdermal.

In these systems, the combinations of polymer matrices and bioactive agents chosen must allow for the drug to diffuse through the pores or macromolecular structure of the polymer upon introduction of the delivery system into the biological environment without inducing any change in the polymer itself [20]. Environmentally responsive systems [Appendix K] when in contact with a particular biological environment, release agent or agents in a stable way based on the kinetics of osmolality. An example of this type of mechanism is a swelling-controlled release system. These systems operate by absorbing water or other body fluids, which induces swelling, causing the dilution of the active agent and the enlargement in the size of the polymer mesh. Diffusion then takes over as the means of drug release. Figures 1.4(a) and 1.4(b) are examples of these types of devices for reservoir and matrix systems, respectively [20]. The theory behind this particular system is based on hydrogels, polymers that swell without dissolving in aqueous solutions. At equilibrium, hydrogels comprise 60-90% fluid and 10-30% polymer.

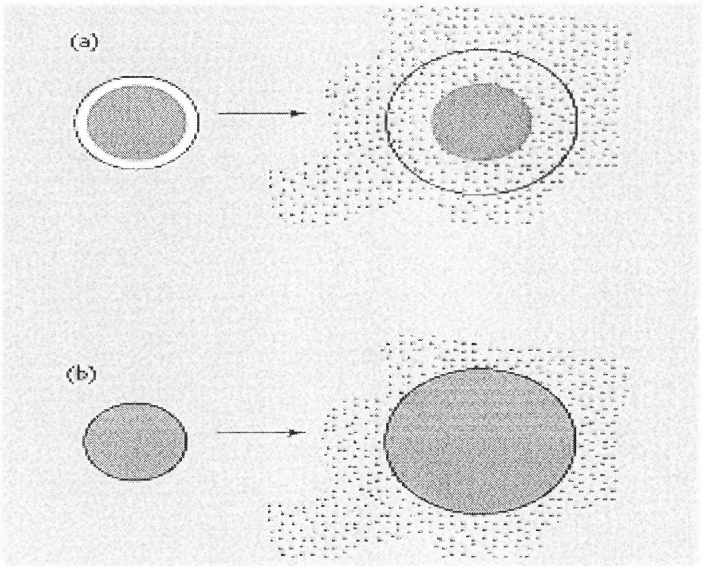

Figure1.4 Environmentally responsive systems (a) reservoir, (b) matrix in swelling-controlled release systems.

The onset of swelling is not just dependent upon contact with a particular environment, but also with changes in the environment. Changes in the environment include temperature, pH, ionic strength, introduction of ionic groups into the environment, ion exchange, variations of diffusion coefficients, and enzymes or other biological elements that can induce shrinkage or swelling. Hydrophilic excipients can be used to accelerate the release of drugs, though they may also increase the burst effect (release of active agent at one time) [18].

The simplest environmental design relies on the difference in pH values, where at high pH values, the system swells and at low values it collapses. The swelling, induction of high pH values triggers the drug release and low pH values arrests release. A number of these environmentally sensitive or "intelligent" hydrogel materials are listed in [Appendix K]. For most of these polymers, the structural changes are reversible and repeatable upon additional changes in the external environment, as illustrated in Figure 1.5 [20]. The drug release mechanism of the system in Figure 1.5 is based upon the swelling of the polymer. Swelling is triggered by an increase in pH value and is ideal for oral delivery where release occurs in the upper small intestine where the pH values are high and not in the stomach where pH values are low.

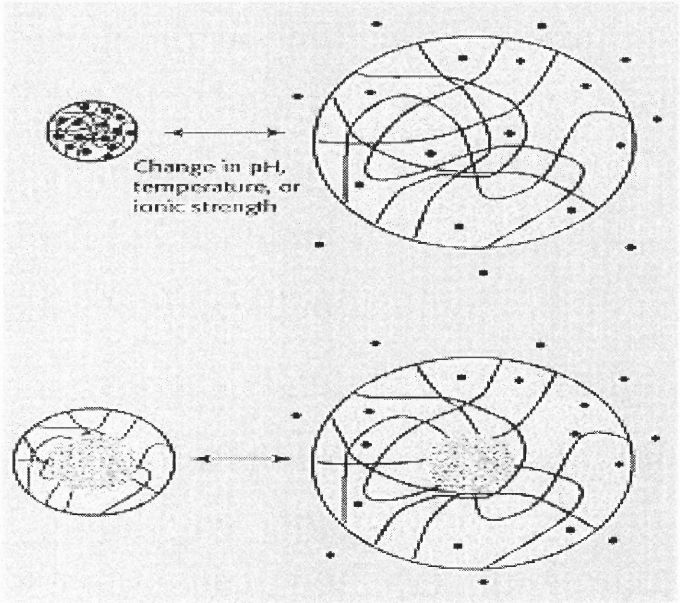

Figure 1.5 Basic changes in polymer structure for environmentally sensitive systems due to swelling.

Contrary to the design of the swelling systems are the biodegradable systems. Biodegradable systems manipulate natural biological processes to degrade the polymer, therefore releasing the drug that was trapped in or on the polymer. In such systems, the chemical structure of the system changes, and the release rate is often governed by the degradation rate in some relationship. Most biodegradable polymers are designed to degrade via the hydrolysis of the unstable polymer chains as soon as they come into contact with water. In the simplest mechanism of chemical hydrolysis, water penetrates the bulk, preferentially attacking the chemical bonds in the amorphous phase and converting long polymer chains into shorter water-soluble, biologically compatible compounds. For some polymer materials such as polylactides, polyglycolides, and their copolymers, the polymers will break down to lactic acid and glycolic acid, enter the Kreb's cycle, and be further broken down into carbon dioxide and water and excreted out

of the body by normal biological processes. Since degradation initially occurs in the amorphous phase, the reduction in molecular weight does not affect physical properties or functionality of the device.

The device is held together by the crystalline regions and remains intact until the degradation reaches a critical point. Homopolymers (polyglycolic acid and polylactic acid) are crystalline, densely packed and able to hinder hydrolytic attack, unlike copolymers, which are amorphous. For amorphous polymers, a hydrophobic layer (a copolymer of lactide, glactide, and calcium stearate) on the surface can be generated, forming an absorbable, adherent, non-flaking lubricant which repels water (molecules cannot reach chain segments in amorphous areas to initiate hydrolysis), slows absorption, and improves the retention of tensile strength [17].

Once the device is broken down, the fragments are further reduced to simple compounds due to enzymatic and metabolic affects. When such an action occurs where there is a rapid loss of polymer mass (the rate at which water penetrates the device exceeds that at which the polymer is converted into water-soluble materials), it is called bulk erosion [16]. Through bulk erosion, the polymer degrades in a fairly uniform manner throughout the matrix, or by surface degradation as in such materials as polyanhydrides and polyorthoesters. In surface degradation, the release rate is proportional to the surface area of the drug delivery system, resulting in a slower rate of conversion of the polymer into water-soluble materials. A hydrophobic polymer whose chemical bonds are highly susceptible to hydrolysis can experience a form of surface degradation, but is often referred to as bioerosion [16]. Figure 1.6(a) illustrates bulk erosion, and Figure 1.6(b) shows surface degradation.

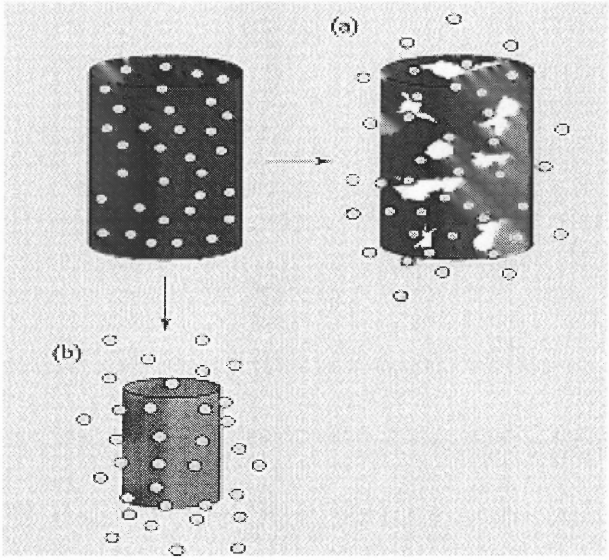

Figure 1.6 (a) Bulk erosion drug delivery, (b) surface degradation for drug release.

Microparticles are an example of bulk erosion systems, used most commonly in oral delivery systems and subcutaneously injected delivery systems. Microparticles of poly (lactide-co-glycolide) (PLGA) can be prepared in a fairly uniform manner to provide essentially nonporous microspheres [Figure 1.7] and reduce to fragments by bulk hydrolysis [Figure 1.8] (example, are of a 75:25 lactide:glycolide PLGA microparticle after 133 days of degradation in water) [20].

Analysis of polyorthoester (surface-eroding polymers) rods after 9 and 16 weeks of implantation in rabbits shows significant surface degradation, but the core of the drug delivery system remains intact [Figure 1.9] [20].

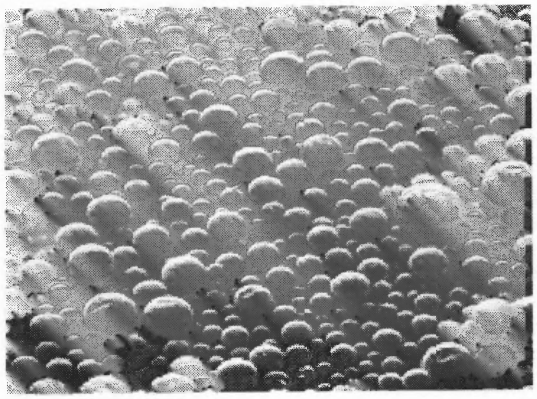

Figure 1.7 Microspheres of 60 lactide:glycolide PLGA.

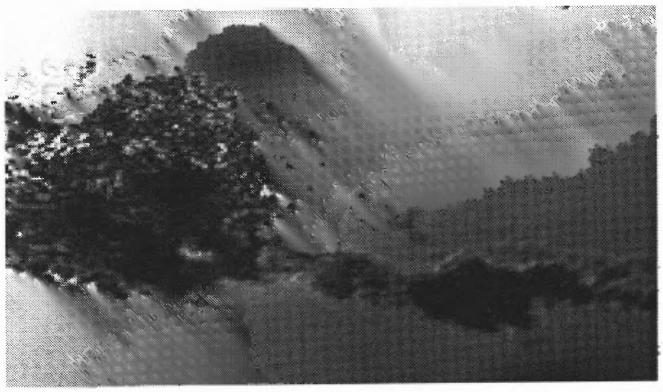

Figure 1.8 75:25 lactide:glycolide PLGA microparticles by bulk hydrolysis.

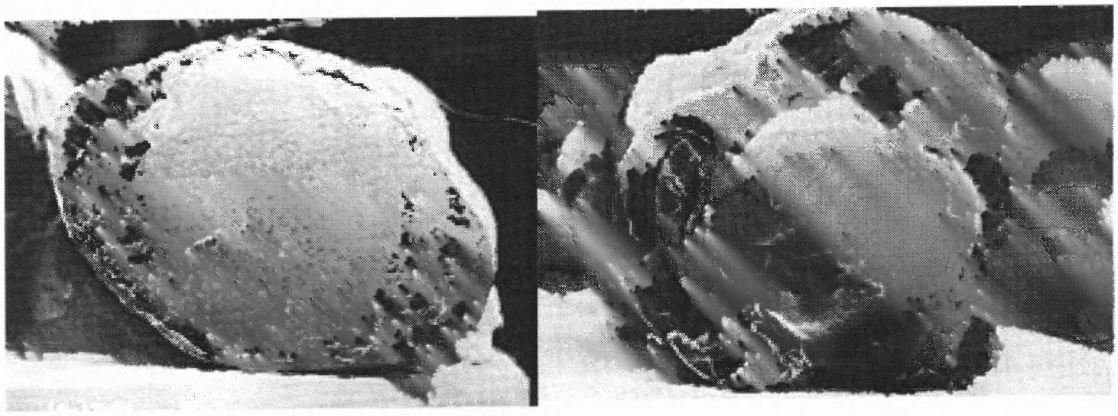

(a) (b)

Figure 1.9 (a) surface erosion of polyorthoester rods after 9weeks and (b) 16weeks.

1.2.6 DLPLGA Characteristics

Poly-glycolic acid (PGA) [Figure 1.10] is the simplest linear aliphatic polyester, with a melting point of 220-225°C and a glass-transition temperature of 35-40°C due to its high crystallinity (45-55% crystalline). Such high crystallinity prevents solubility in most organic solvents with the exception of highly fluorinated organics such as hexafluoroisopropanol. Ring-opening polymerization yields high-molecular-weight materials, with approximately 1-3% residual monomer present and dimerization of glycolic acid results in glycolide monomers. Unlike the slow absorption of Poly-lactic acid (PLA), PGA is absorbed within a few months postimplantation due to greater hydrolytic susceptibility [15].

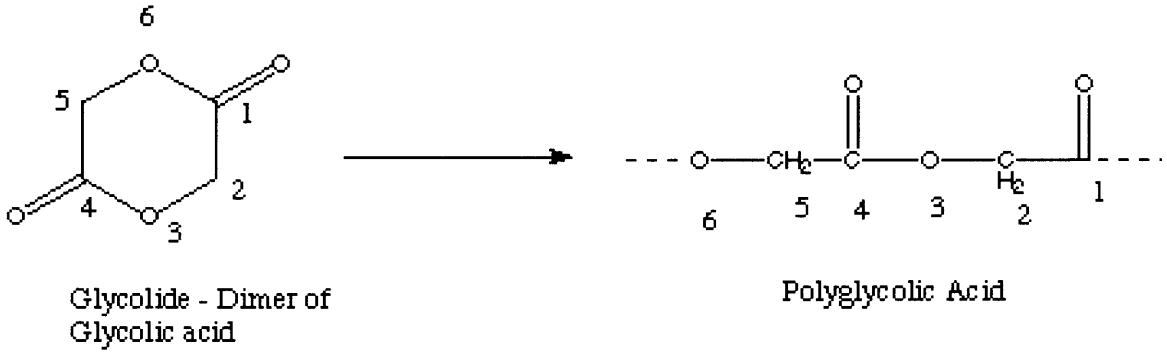

Figure 1.10 Ring opening polymerization of glycolide dimer to polyglycolic acid.

In vitro experiments concluded that enzymes, buffer (moisture), pH, annealing treatments, and gamma radiation enhance degradation of PGA, therefore low humidity ethylene oxide gas sterilization procedures and moisture-proof packaging are utilized. Gamma irradiation can be used when the onset of degradation is desired at a faster rate.

PLA (poly-lactic acid) [Figure 1.11] is prepared from the cyclic diester of lactic acid (lactide) by ring opening polymerization. Lactic acid exists as two optical isomers or enantiomers (D and L), the L-enantiomer (crystalline) occurs in nature, and a D, L racemic mixture (LPLA, a semicrystalline polymer) can be made by synthetic preparation of lactic acid.

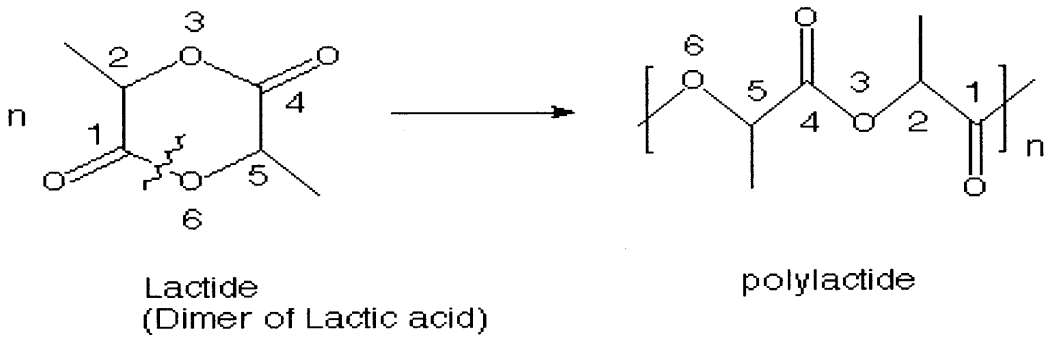

Figure 1.11 Ring opening polymerization of lactide to polylactides.

Poly-L-lactide is about 37% crystalline with a melting point of 175-178°C and a glass transition temperature of 60-65°C [17]. Electrospun fibers from L-polylactide (mp. 170 C) have high crystallinity, whereas poly DL-lactide electrospun fibers are amorphous (no reported melting point [mp]). Poly L-lactide is more resistant to hydrolytic degradation than the amorphous DL form, due to its crystalline nature, which exhibits high tensile strength and low elongation, resulting in a high modulus (more suitable for load bearing devices). DLPLA is an amorphous polymer exhibiting a random distribution of both isomeric forms of lactic acid, is unable to arrange into an organized crystalline structure, and has lower tensile strength, higher elongation, and faster degradation time (ideal for drug delivery systems).

Carboxyl-ended PLGA polymers degrade slower than hydrophobic end-capped PLGA polymers. Polylactides are more hydrophobic; therefore take a longer time to degrade, unless plasticized with triethyl citrate (producing a less crystalline, less tensile, faster degrading material [17]). Time required for poly-L-lactide implants to be absorbed depends on polymer quality; processing conditions, implant site, and physical dimensions of the implant [15]. In vivo studies in rats showed an absorption time of about 1.5 years for 50-90 mg samples of radiolabelled poly-DL-lactide implanted in the abdominal wall [15]. In the radiolabelled implants, metabolism of the polylactides resulted in excretion primarily via respiration (CO2) and exposure to gamma radiation showed a decrease in molecular weight (MW). The degradation time of LPLA takes more than two years to be completely absorbed, much slower than DLPLA. Copolymers of L-lactide and DL-lactide have been prepared to disrupt the crystallinity of L-lactide and accelerate the degradation process [17]. The rate of degradation of lactide based polymers and in general all hydrophobic degradable polymers, depends on chemical composition, crystallinity, and hydrophilicity. Degradation by chemical composition depends on the rate of degradation of the bonds present (Anhydrides faster than esters, faster than amides). The higher the crystallinity and hydrophobic nature (versus hydrophilic), the slower the degradation rate. Schwendeman and Zhu (Zhu and Schwendeman, 199 et al., 2000) have shown that by incorporating basic salts as excipient polymeric microspheres, the stability of the incorporated protein improved, with the side effect that these basic salts slowed degradation time.

Amorphous copolymers have a compositional range between 25-70 mole percent glycolide, where pure polyglycolide is about 50% crystalline and pure poly-L-lactide is

about 37% crystalline. There is a disruption of the regularity of the polymer chain by the other monomer in a racemic mixture. A copolymer of 50% glycolide and 50% DL-lactide degrades faster (in 50-60 days) than either polymer independently, or copolymer with differential percentages of either polymer. A copolymer of 90% glycolide and 10% L-lactide was developed by Ethicon under the trade name Vicryl, which absorbs within 3-4 months but has a slightly longer strength-retention time [17]. In general, the 65:35, 77:35, and 88:15 D, L-lactide/glycolides have progressively longer *in vivo* lifetimes, with the 88:15 lasting about 150 days in vivo, whereas poly (D, L-lactide) requires about 12-16 months to biodegrade completely, and poly (L-lactide), being more crystalline and less hydrophilic, can be found in vivo in about 1-1/2 to 2 years (Cutright et al. 1974, Hausberger & De Luca 1993, Holland et al. 1986, Matsusue et al. 1992, Pistner et al. 1993, Yamaguchi & Anderson 1993) [19]. Factors that affect the performance of biodegradable polymers (in general) are hydrophilicity, crystallinity, melt and glass-transition temperatures, molecular weight, molecular-weight distribution, end groups, sequence distribution (random versus blocky), and presence of residual monomer or additives. The most common functional groups with these characteristics are esters, anhydrides, orthoesters, and amides. A more hydrophilic backbone, less crystallinity, more porosity, more hydrophilic endgroups, more reactive hydrolytic groups in the backbone, and smaller device size are factors that reduce degradation (accelerates the action of) time.

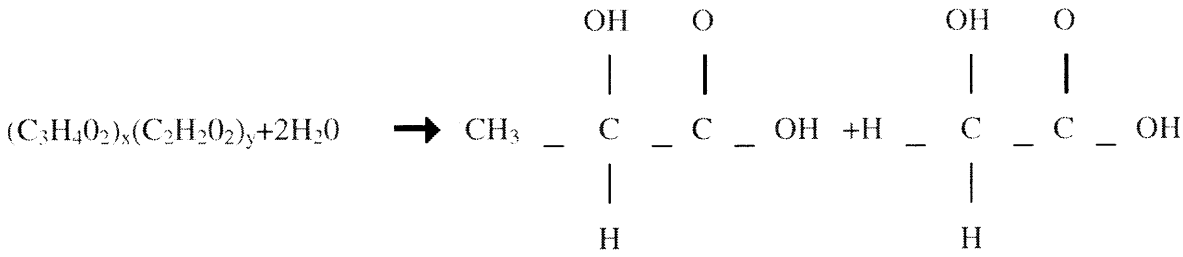

Figure 1.12 Degradation and metabolization of PLGA.

Medisorb polymers (polymers used in this research, Appendix C, D, E, G, H, I, J) are biodegradable polyesters that undergo resorption of physiological conditions at varying rates depending on chemical characteristics of the polymer and attributes of the device. Degradation occurs via hydrolysis of ester linkages, followed by gradual erosion of the device. Like their general counterparts, the final products of PLG degradation are lactic acid and glycolic acid, water soluble, non-toxic products of normal metabolism, that are either or further metabolized to carbon dioxide and water [Figure 1.12].

CHAPTER 2

ELECTROSPINNING TECHNIQUE

Electrospinning is the process of charging a drop of polymer in solution with tens of thousands of volts undergoing metamorphosis from a Taylor cone into strands of polymer on the nanoscale size (by spraying). Electrostatic charging of the fluid at the tip of the nozzle results in the formation of a Taylor cone, in which multiple filaments are ejected to produce nonwoven materials that have a porosity factor, high surface area, and fineness and uniformity. The filaments are the result of the jet accelerating and thinning in the electric field, a process known as "splaying." Studies suggest that the most important element operative during electrospinning is the rapid growth of a non-axisymmetric, or "whipping," instability that causes bending and stretching of the jet [Figure 2.1(a)] [2]. The unstable region of the jet [Fig. 2.1 (b)] viewed at exposure times down to the millisecond, has the appearance of an "inverted cone," while in [Fig 2.1(c)], using high-speed photography, a single, rapidly whipping jet was observed by Shin et al. The whipping frequency is so fast that the jet appears to be splitting into multiple filaments [2].

It was demonstrated by Hohman et al. that there are three different modes which are unstable: (1) the Rayleigh mode, which is the axisymmetric extension of the classical Rayleigh instability when electrical effects are important: (2) the axisymmetric conducting mode; and (3) the whipping conducting mode. (The latter are dubbed "conducting modes" because they only exist when the conductivity of the fluid is finite [3].) Hohman et al. demonstrated that the dominant instability strongly depends on the

fluid parameters of the jet (viscosity, dielectric constant, and conductivity) and also the static charge density on the jet.

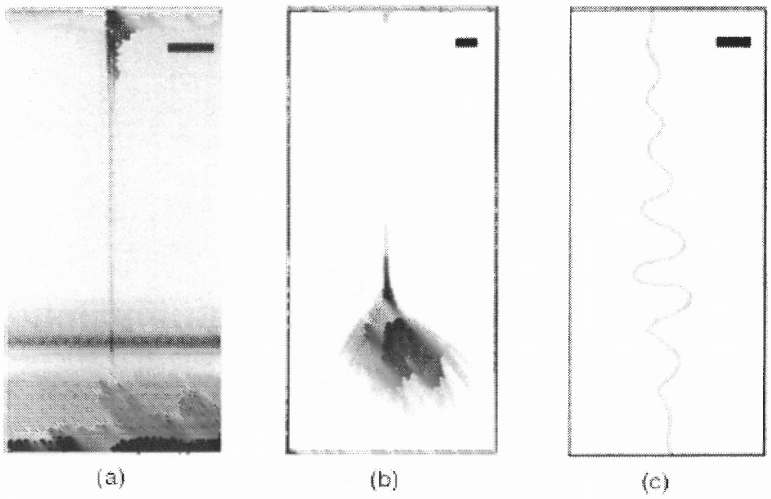

Figure 2.1 (a) Fluid jet, (b) Splaying, (c) Whipping motion.

The actual process of electrospinning involves applying a high voltage to a syringe (or some form of conduit) and pumping a polymer solution through it at a steady rate. Nanofibers of polymer are collected as a nonwoven sheet on a grounded plate below the capillary [Figure 2.2].

In the absence of an electric field, the fluid forms a drop at the exit of the conduit; its size is determined by surface tension, distance between conduit and grounded plate, and pumping rate. When an electric field is applied, a charge is introduced to the fluid that quickly relaxes the fluid surface, creating a tangential stress, resulting in the deformation of the droplet into a conical shape (Taylor cone) [5].

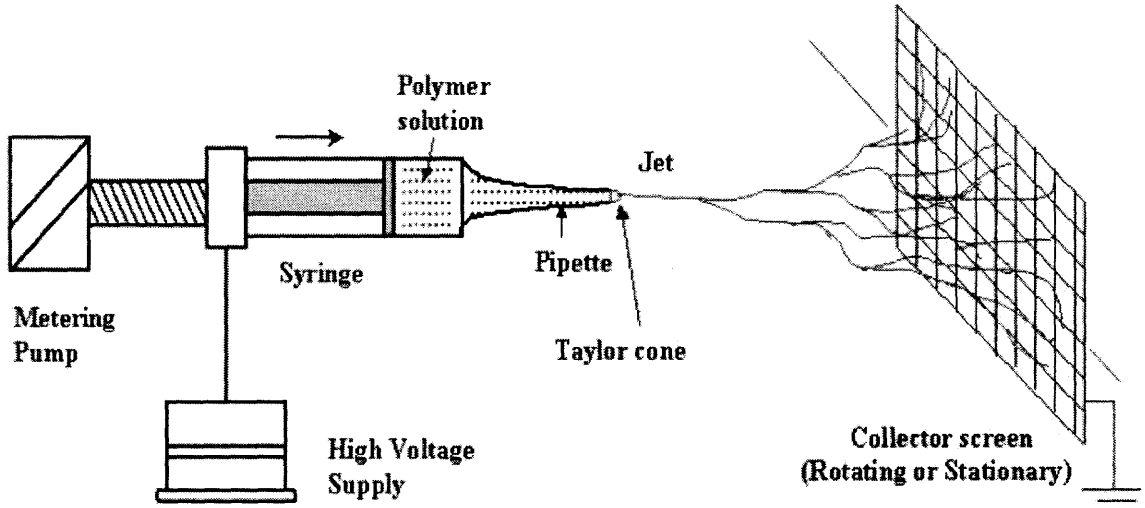

Figure 2.2 Electrospinning setup.

Hohman et al. demonstrated that when the electric field exceeds the critical value needed to overcome the surface tension, the apex of the cone ejects a fluid jet, where at low viscosity, the jet breaks up into droplets, while at higher viscosity the jet forms a continuous, small-diameter filament. Droplet formation depends on viscosity, therefore the solution or melt viscosity is shown to affect both the processing window for electrospinning and the diameter of the fiber [4]. Electric field parameters also affect fiber morphology.

Rutledge and Shin discovered that the small-diameter fibers generated when the filament became unstable and split into smaller filaments (splaying), was actually the main filament whipping around, stretching into a single long fiber. They demonstrated this concept with poly-ethylene oxide (PEO) solutions of varying concentrations (i.e. viscosity) in water, with KBr to adjust the fluid conductivity. The results of their experimental analysis was that the solution flow rate and the electric field strength were the key operating parameters determining the jet's stability and that the measured current

of the jet provided information about the surface charge density on the jet [5]. Larrado and Manley determined that doubling the applied electric field decreased the fiber diameter by roughly half. However, Baumgarten showed that the diameter of the jet reached a minimum after an initial increase in field strength and then became much larger with increasing fields, an effect caused by the pumping rate [4]. Therefore he concluded that increasing the field does increase the electrostatic stresses, creating smaller diameter fibers, but it also draw more material out of the syringe [4].

In general increasing the grounded surface distance, decreases fiber diameter; increasing electric potential (kV), decreases fiber diameter to a critical point; increasing flow rate, increases fiber diameter; increasing concentration wt%, increases fiber diameter, and decreasing the conduit size decreases fiber diameter.

CHAPTER 3

MATERIALS

The DLPLGA (D-L-Poly-Lactic-Glycolic-Acid) polymer in ratios of 75/25, 80/20, and 85/15 was obtained from Alkermes in 50gram packages (per ratio). Due to their highly hydrolytic nature, the polymers were kept in airtight bags in the freezer. The samples of 75/25 and 85/15 DLPLGA are GMP approved, but the 80/20 DLPLGA was not.

Obtained from the Medisorb® Polymer Products (division of Alkermes) was the following product information [Table 3.1]:

Biodegradation rates depend on: device geometry, porosity, lactide:glycolide ratio, MW/inherent viscosity (IV)/Polymer end groups, and crystalline vs. amorphous character.

Table 3.1 Product Information

85/15 DL 2A	
85 Mole % DL Lactide, 15 Mole % Glycolide	Acid End Group
High IV 0.66-0.80 (DL/G)	Degradation range of 5-6months
Low IV 0.50-0.65 (DL/G)	
75/25 DL C01	
75 Mole % DL Lactide, 25 Mole % Glycolide	Custom 01
High IV 0.66-0.80	Degradation rate 4-5 months
Low IV 0.50-0.65	

Standard end group is lauryl ester (capped), polymer identifier marked with either A, M, or C.

A - polymers contain a free carboxyl end group (uncapped)

M - polymers contain a methyl ester end group (capped) which lower inherent viscosity with a higher Tg

C - polymers are custom polymers in which the end group will vary depending on the batch ordered. The C designation may also include polymer that has a targeted Inherent Viscosity Range that does not comply within the Standard Inherent Viscosity Specifications detailed below.

Target Polymer Inherent Viscosity (IV) Specification Ranges

Polymer Ratio	Polymer Identifier	IV (DL/G)	End Group
ALL	Low IV	0.50 - 0.65	Ester
ALL	High IV	0.66 - 0.80	Ester

The molecular weight of the 75/25 DLPLGA was 113Kd, 123.6Kd for the 85/15 sample, and 104Kd for the 80/20 DLPLGA sample. The molecular weight was important in determining how well the polymer would go into solution and an estimate on how the electrospinning samples would turn out (diameter size).

Other important characteristics of the polymers are found in Appendix C, E, G, H, I, J.

The solvent used was Tetrahydrafuran (THF) because it was one of few solvents that could dissolve both the DLPLGA and the BCNU without disrupting the functionality of either the polymer or the drug [Appendix D, F].

The drug of choice was referred by Charles J. Prestigiacomo, MD, from the neurosurgery department at the University of Medicine and Dentistry of New Jersey (UMDNJ). Since BCNU is a common chemotherapeutic agent in the treatment of various types of brain tumors, significant amounts of data regarding its pharmacokinetics and bioavailability in differing preparations are readily available for comparison, making

this the ideal choice to test the ability to deliver chemotherapeutic agents via nanofiber technology. As mentioned in the section 1.2.3 Pharmacokinetics of BCNU, BCNU was the drug of choice when Gliadel marketed their biodegradable, implantable wafers to prevent tumor reoccurrence.

The drug was obtained from the pharmacy at UMDNJ in powder form for dissolution with the polymer in the solvent THF.

Proprietary Name: BCNU

USA Brand Name: Sterile Carmustine, FDA approved chemotherapy agent, NSC #409962 (1977)

Active Agent: Carmustine

Common Names: BCNU, BiCNU, Carmustine,

Classification: Alkylating Agent, Nitrosurea

Average Patient Dosage: as a single chemotherapeutic agent 150-200mg/m2 every 6 weeks

Potential Side Effects: Bone Marrow Suppression, Anemia, Diarrhea, Low White Blood Counts, Low Platelet Counts, Kidney Damage, Lung Damage (Pulmonary Toxicity), Mouth Soreness, Swallowing Difficulties [21].

Must be stored in refrigerator before use and decomposes at 86.6-86.9 °F. Use within 8 hours at room temperature and protect from sunlight.

After intravenously administered, BCNU can cross the blood brain barrier due to its high lipid solubility and lack of ionization, and is rapidly degraded with no intact drug detectable after 15minutes [21].

Research analysis showed that the toxicities of BCNU are due to metabolites; approximately 60-70% of a total dose is excreted through urine within 96hours and approximately 10% as respiratory CO_2. The remaining 20-30% is unknown [21].

The Electrospinning Assay was obtained from multiple sources and was constructed by Shobana Shanmuga Sundaram of the Medical Device and Concept Lab at the New Jersey Institute of Technology (NJIT). The voltage source, Gamma High Voltage Research (Ormond Beach, FL) of 25kV was used to apply electric field and prevent droplets.

The syringe was from Fisher Scientific, of sizes 22-16 gages, where a 20 (outer diameter of 0.036" and inner diameter of 0.023") and 22 gage (outer diameter of 0.028" and inner diameter of 0.016") was used.

The screens, plastic wrap and glass specimen slides were used as the collecting surface. Most of the screens and plastic wrap were obtained from the local grocery store or hardware store. Fisherbrand colorfrost microscope slides (size 25 x 75 x 1mm) from Fisher Scientific (Pittsburg, PA) were used.

CHAPTER 4

METHODOLOGY

The research was split into three distinct procedures: (1) the Electrospinning process, (2) Characterization of the polymer as electrospun fibers using analytical techniques and instruments, and (3) Electrospinning and characterization of the drug and polymer complex.

4.1 Electrospinning Process

(1) Prepare the polymer solution - DLPLGA was dissolved in THF to make 6-wt%, 10-wt%, and 15-wt% solutions.

(2) Solution took 30-45minutes to completely dissolve the polymer (using a magnetic stirring rod and mixing apparatus) and then was let to stand overnight.

(3) The syringe with a 20 gage or 22-gage diameter needle of polymer solution was prepared for the Syringe pump.

(4) A non-conducting plastic tube was connected between the syringe and the needle

(5) The needle was placed horizontally and perpendicular to the vertical surface (ex. wire screen, plastic film or glass specimen slide) to collect the electrospun nanofibers. The distance between the tip of the needle and the vertical surface was between 15-20cm.

(6) The electrode wire was connected to the syringe needle, the vertical surface grounded.

(7) Attach the syringe pump to conduit and leaked some of the solution out through the syringe.

(8) When the solution started to flow out of the syringe needle, sometimes a bead of solution would form at the tip, blocking the flow. A pair of tweezers was used to clear the obstruction.

(9) Once the flow of the solution was constant (syringe pump set at 0.103ml/min), the power supply was turned on and voltage set at 25kV.

(10) After electrospinning all the samples, the power supply was turned off.

(11) The syringe pump was turned off.

(12) The electrospun sample was then labeled and prepared for characterization and microscopy.

(13) All materials were then cleaned.

4.2 Characterization of the Electrospun Fibers

Differential Scanning Calorimetry (DSC – TAQ100) is used for thermal analysis by measuring stability through heat flow (can either be a heat/cool/heat process or a heat process).

(1) Prepare electrospun fiber sample by cutting a piece of the fiber mat from the glass slide.

(2) Using DSC computer software, activate the cooler. Turn on DSC gas.

(3) Using an aluminum pan, tare the pan and weigh fiber sample. Place a lid on the sample pan and crimp the lid onto the pan.

(4) Using the Wizard option on the control bar, set parameters for sample (ex. temperature scale, rate of temperature change, sample weight).

(5) Run sample, graph, and save graph on file.

(6) Unload sample, turn off DSC gas and deactivate the cooler.

Thermal Gravimetry Analysis (TGA - TAQ50) using weight as a measure of temperature. With increasing temperature, residual mass is lost.

(1) Turn on TGA gas.

(2) Using TGA sample loading dock, push furnace button.

(3) Push sample button to obtain access to the balance. Do not touch balance.

(4) Once the weigh tray is detached from the balance, tare the weigh tray with empty aluminum pan.

(5) Load sample onto the pan. Using the TGA computer software, attach weigh tray to the balance and run sample.

(6) Graph sample and save on file.

(7) Unload sample, turn off TGA gas.

Scanning Electron Microscopy (SEM) is an electron microscope that uses a beam of focused electrons across an object to produce a high-resolution (three-dimensional) image.

1 Sign the log in book.

2 Using the SEM computer software, log in, record initial parameters, and check with log in book.

3 Prepare sample, using tweezers, gloves, and loading disk.

4 Click vent (Nitrogen gas) to get to atmospheric pressure in sample chamber to load sample.

5 Load sample (still wearing gloves) and press pump. Make sure door to sample chamber is shut. At this point the gloves can be taken off.

6 Using right joint stick, bring stage up to 11mm (or two finger width) distance between the sample and the power piece.

7 Apply voltage. Using tool bar, use center point locator, magnification, focus, and stigmation to obtain the sample area of investigation.

8 Scan sample area under investigation and save in file.

9 Turn off voltage and write down final parameters in log in book.

10 Turn vent on, and unload sample (wear gloves).

11 Turn pump on and log off software.

4.3 Electrospinning and Characterization of Drug and Polymer Complex

Characterization was done with the SEM to determine if the drug had any affect on the polymer diameter or morphology.

DSC was run to see any changes in temperature based on the presence of the drug. TGA was run to determine if the amount of mass loss in the polymer sample and at what temperature degradation might take place.

All three would determine if the process of putting the drug on the polymer worked. It was the goal of this research to see if the drug was present in the polymer. Further analysis will have to be done on the amount, release rate, and functionality of the drug in the electrospun polymer. Also whether the electrospinning had any affect on drug performance.

CHAPTER 5

RESULTS

Choosing the solvent was a crucial step in the process. In order train with the electrospinning technique, methylene chloride (MeCl) was used as the solvent for a 75/25 DLPLGA 10wt% practice sample. This was not the solvent to be used for the drug delivery system (which was chosen to be Tetrahydrofuran [THF]). By adjusting the technique and obtaining adequate fibers, the actual experimental samples were made.

When using THF, a highly volatile solvent, certain methods needed to be introduced. Latex gloves, eyeglasses, mask (covering nose and mouth), and a fume hood (where all the mixing occurred) was used. While mixing the polymer and the solvent, using 100ml of solvent and various grams of polymer (10grams for 10wt%, 6grams for 6wt%, 15grams for 15wt%, and 8grams for 8wt%), due to the nature of the solvent, 5% (by volume) of solvent slowly dissipated from a 100ml solution. Once the polymer was mixed, the samples solutions were sealed to prevent further evaporation of solvent (therefore creating a more concentrated solution than originally intended). After letting the solvent settle overnight, the electrospinning process commenced.

The samples made were a 10wt% of 80/20 and 85/15, and a 6wt% of 80/20, 85/15, and 75/25 polymer. In the initial stages of the electrospinning process, all slides of various sample weight solutions were absent of fibers (only droplets were present when specimens were evaluated with the optical microscope (OM). One expectation for this observation is that the solution was not viscous enough and needed a longer time to settle. After a few days (3-5 days), the 80/20-10wt% demonstrated fibers on the slide with multiple beads in the strands (using the OM) and the 85/15-10wt% showed a few strands,

but mostly atomized droplets (using the OM). After a two-week period, the 80/20-10wt% was completely solid, where the THF completely evaporated. The 85/15-10wt% solution was had very high viscosity and therefore could not undergo the electrospinning process. The 85/15-6wt%, 80/20-6wt%, and 75/25-6wt% still had low enough viscosity to electrospin. At the two-week period, the 85/15-6wt% seemed really viscous (not quantified, just a physical observation) and there was some doubt as to whether it would pump through the syringe. Surprisingly, the solution provided a small diameter fiber network with no beading. Under optical microscopy, there were sections of the fiber that were larger and flatter while other sections appeared round and thinner. The polymer samples proved to be sustained at a max time limit of two weeks, in comparison to the MeCl, which had only a one-week longevity period, but produced fibers within a day of mixture. This may indicate that the entanglement of the polymers can be sustained for a certain range of time depending upon the solvent used. The eventual hardening of solution is due in part to both entanglement properties and evaporation.

In the process of spinning nanofibers, initially a 20gauge needle was used, but a 22gauge proved useful in creating smaller diameter fibers and providing extra pressure at the point of ejection of the fluid jet. Interestingly, the smaller needle diameter provided by the 22gauge allowed for fiber formation to occur in sample solutions that were creating only droplets with the 20gauge. Smaller diameter fibers were also created by increasing the distance between the tip of the fluid jet and the screen from 15mm to ~25mm. Gradually as time increased, with the fibers undergoing entanglement, there was a higher probability for fiber formation, and an increase in density of fiber samples (observed under the OM [Table 5.1]).

The 80/20 10wt% samples on 11/25/03, observed under the OM, defined a distinction between beading and density. The 20gauge electrospun sample looked as if there were more beads intertwined in the fiber network than the 22gauge. This was due to the dense network (more fibers per um^2) of fibers by the 20gauge than the 22gauge. The 22gauge did not produce a thick fiber mat (sheet of fiber sample on slide), therefore beading seemed noticeably less than in the 20gauge slide. In comparison though, based on the um^2 and beading average, the two samples produce the same results.

Table 5.1 Fiber Observations Using OM

Date	Polymer	Wt%	Needle size	Description
11/19/03	80/20	10wt%	20gauge	Fibers present, but lots of beads
11/19/03	80/20	6wt%	20gauge	Droplets
11/19/03	85/15	10wt%	20gauge	Droplets
11/19/03	85/15	6wt%	20gauge	Few fibers, mostly droplets
11/19/03	75/25	6wt%	20gauge	Droplets
11/20/03	80/20	10wt%	20gauge	Lots of fiber formation with beading, formation in 3D, fiber diameter more uniform, beads encapsulated polymer/solvent
11/20/03	80/20	10wt%	22gauge	Fibers with lots of droplets, fibers not densely packed, organized pattern appearing, uniform diameter
11/20/03	80/20	6wt%	20gauge	Droplets
11/20/03	80/20	6wt%	22gauge	Some fibers, some droplets
11/20/03	85/15	10wt%	20gauge	Droplets
11/20/03	85/15	10wt%	22gauge	Few fibers, mostly droplets
11/21/03	80/20	10wt%	20gauge	Large amounts of fiber, scattered beading, uniform diameter
11/21/03	80/20	10wt%	22gauge	Fibers with beading
11/21/03	80/20	6wt%	22gauge	Fibers with beading

Table 5.1 Fiber Observations Using OM (Continued)

11/21/03	85/15	10wt%	20gauge	Fiber formation with beading
11/21/03	85/15	10wt%	22gauge	Fiber formation with beading, not much difference from 20gage
11/21/03	85/15	6wt%	20gauge	Few fiber strands, lots of droplets
11/21/03	85/15	6wt%	22gauge	Few fibers, less droplets
11/25/03	80/20	10wt%	20gauge	Nice fiber network, uniform diameter with beading present
11/25/03	80/20	10wt%	22gauge	Uniform fiber formation, not as dense a sample, beading still exists
11/25/03	80/20	6wt%	20gauge	Droplets
11/25/03	80/20	6wt%	22gauge	Droplets
11/25/03	85/15	10wt%	22gauge	Uniform small diameter, fiber formation with less beading
11/25/03	85/15	6wt%	22gauge	Few fiber formation, some beading, diameter looks smaller than other samples
11/25/03	75/25	6wt%	22gauge	Droplets
11/25/03	Glove	Multi	Multi	Using the sample obtained from the gloves worn, sample on the glove showed a branching network of the fibers, larger diameter than all other samples, and densely packed (3D network)
12/01/03	80/20	6wt%	20gauge	Droplets
12/01/03	80/20	6wt%	22gauge	Droplets
12/01/03	85/15	6wt%	20gauge	Large fiber diameter, branching network, no beading
12/01/03	85/15	6wt%	22gauge	Nice fiber formation, no beading, sections where fiber diameter gets larger
12/01/03	75/25	6wt%	22gauge	Droplets
12/04/03	85/15	10wt%	22gauge	Extremely large fiber diameter, no beads, areas where diameter thick and gel-like
12/04/03	85/15	6wt%	22gauge	Fiber diameter smaller, sections where diameter gets thick and gel-like
12/04/03	75/25	6wt%	22gauge	Droplets

Incidentally, during the electrospinning process on 12/04/03 the sample 85/15-10wt%, an indirect relationship was noted. After turning off the power source and allowing the syringe to be placed on the collecting screen, solution was still electrospinning out. There was a slight attraction that still existed between the needle tip and the grounded collecting surface which induced fibers to form and be pulled from the solution stream (residual pressure within the syringe still existed even when the syringe pump was turned off. The distance between the syringe needle and the grounded surface was about 0.75mm. Since the fibers formed by this method were large enough to be seen by the naked eye (the size of human hair fibers), the actual circular whipping motion of the fiber was observed. Using the OM, the fibers were large in diameter, but still created a pattern similar to what was observed when the power source was on and the distance between the needle tip and the grounded surface relatively large (in comparison). Also, the glove sample (fibers taken from latex glove collected during electrospinning process) was shown to have interesting morphology, a branching network based on all the fibers collecting on one surface (all different ratios and wt%) and interacting (Figure 5.1).

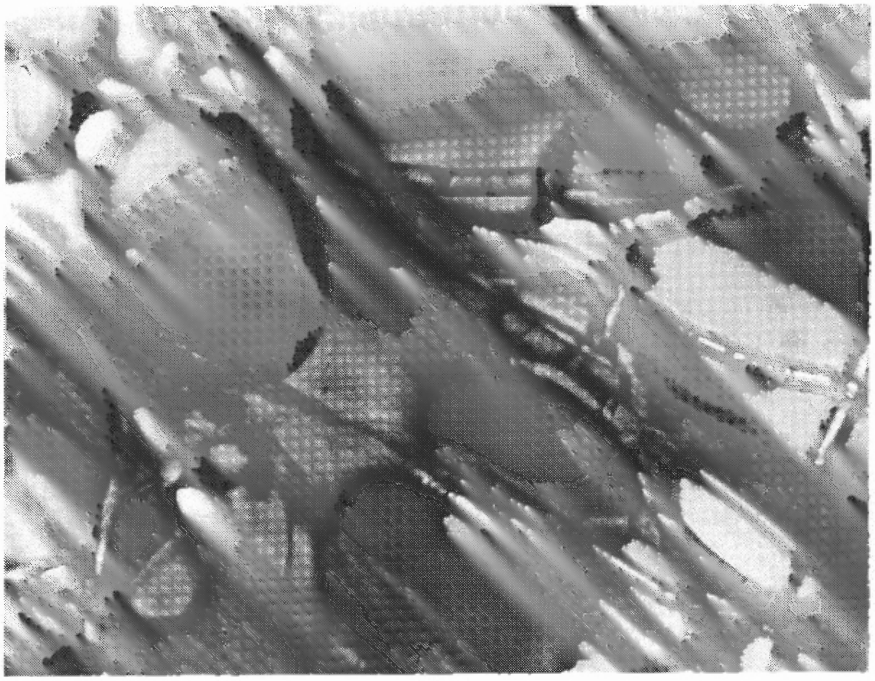

Figure 5.1 Branching morphology observed in glove samples using OM, magnification of 50.

Upon review of the preliminary data from Table 5.1, determining which polymer ratios and weight percentages provided the most uniform and small diameter fibers, samples of 80/20-8wt% and 85/15-15wt% were used for subsequent studies as those specimens that had the possibility of providing the most consistent fiber diameters. Initially, as observed before, the solutions did not spin out nanofibers, but only droplets were present on the slide. After a week, the 80/20-8wt% resulted in some electrospun fibers with a mixture of droplets and beading. The solutions were left open (not entrapped by plastic wrap) in order to speed up the process of evaporation and possible polymer settling. In about one week after mixture, the more concentrated solution (15wt%) had less evaporation than the less concentrated (8wt%). Both solutions started out with 100ml of THF, but after one week, the 85/15-15wt% still had 100ml of solvent, and the 80/20-8wt% had only 50ml of solvent. With the decrease in solution volume, but

not density, the 80/20-8wt% was not actually 8% wt/wt. The 85/15-15wt% spun out the best diameter fibers from the two solutions. The 80/20-8wt% produced a few strands (3-5) but not the same volume as the 85/15-15wt%. Therefore the entanglement process is not a function of increased concentration by evaporation, but by true entanglement. This is proven by the evaporation of about 50% of solution from sample 80/20-8wt%, and the production of a few fibers. Both samples had the same lag-time therefore time is not a factor for comparison.

The best results of the electrospinning process in regards to wt% and polymer ratios of lactide to glycolide were the 80/20-10wt% and the 85/15 6wt%. These two ratios would be used in combination with 50ml of BCNU (including diluent) to test the electrospinning process on the drug.

The normal dosage required for BCNU administered intravenously is between 150-200mg/m^2. Based on the known background information that the electrospun nanofibers have a higher surface to area to volume ratio, and dense volume over a small area (therefore higher concentration of active agent), a third of the dosage (50mg/m^2) was used. After letting the samples rest 18 hours, the solutions were electrospun the next day, with only the 80/20-10wt% plus drug producing fibers. The 85/15-6wt% did not.

The following were all factors that were kept constant: drug (50mg/m^2 of BCNU and diluent), solvent (THF), syringe diameter, thru-put (~25kV), screen distance from syringe (15mm-25mm), and solution lag-time (overnight).

In order to obtain the electrospun fibers with the smallest diameter without the intrusion of droplets intertwined among them the following was considered: (1) the syringe gauge size, the voltage, the concentration of wt% samples, and the distance

between the tip of the syringe and the vertical plate. By keeping the syringe gage small, the voltage large as possible (without having droplets form again due to too high an electric field), the smallest concentration of wt% samples, and increasing the distance between the tip of the syringe and the vertical plate, the fibers below [Figure 5.2, Appendix L] were observed using SEM analysis.

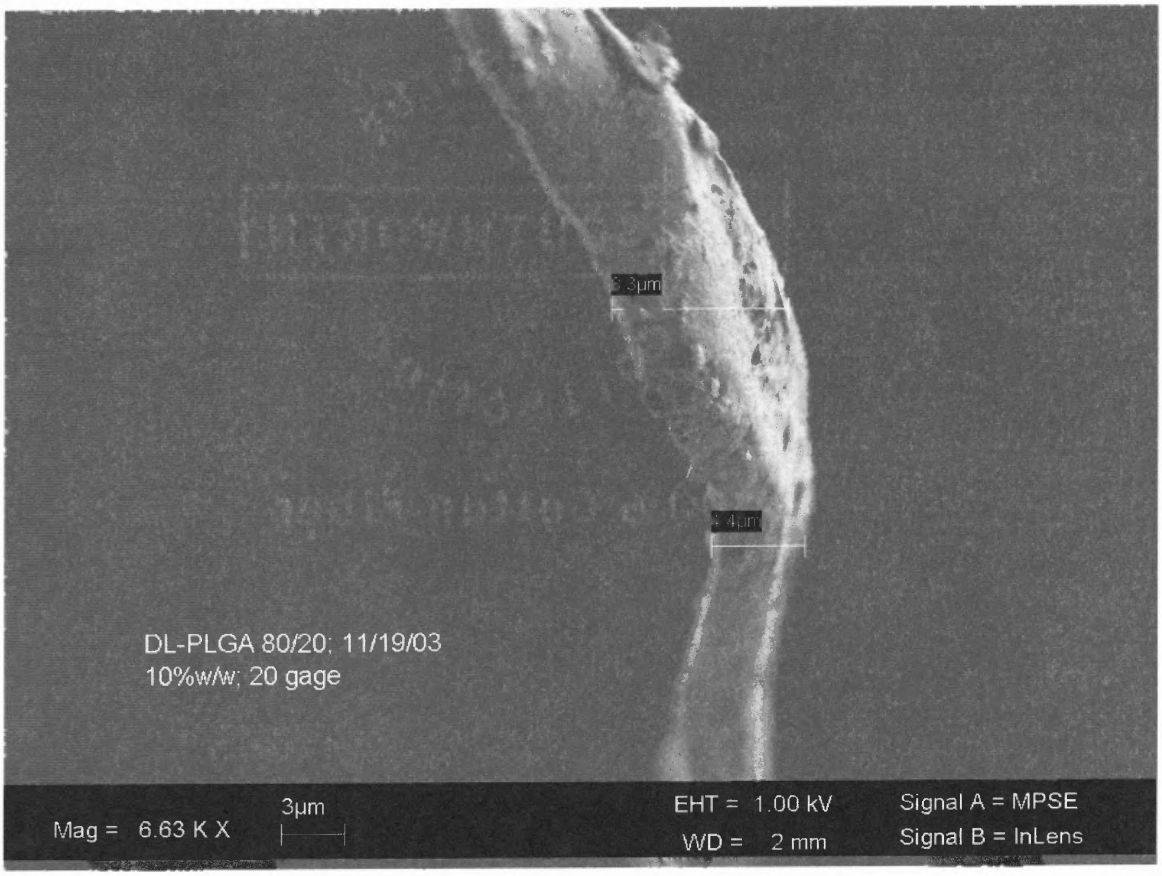

Figure 5.2 (a) 80/20-10wt% 11/19/03 22gauge.

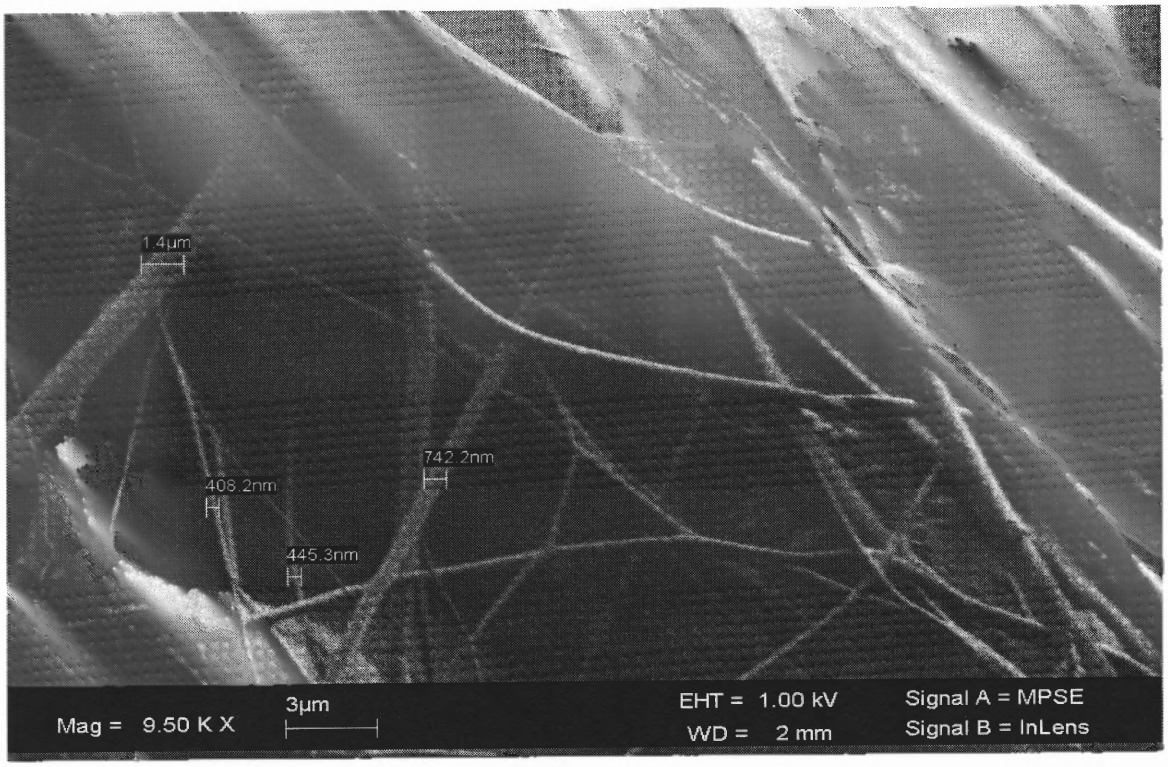

Figure 5.2 (b) 80/20-6wt% 11/20/03 22gauge.

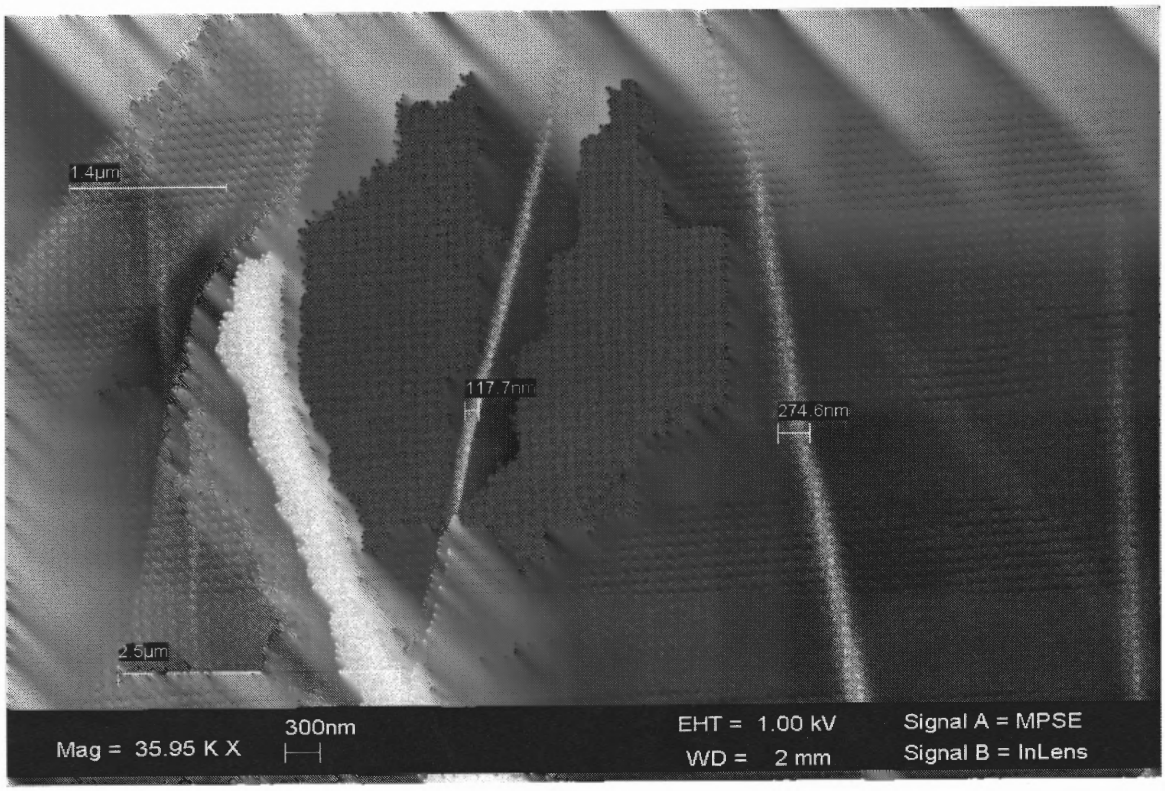

Figure 5.2 (c) 80/20-6wt% 11/20/03 22gauge.

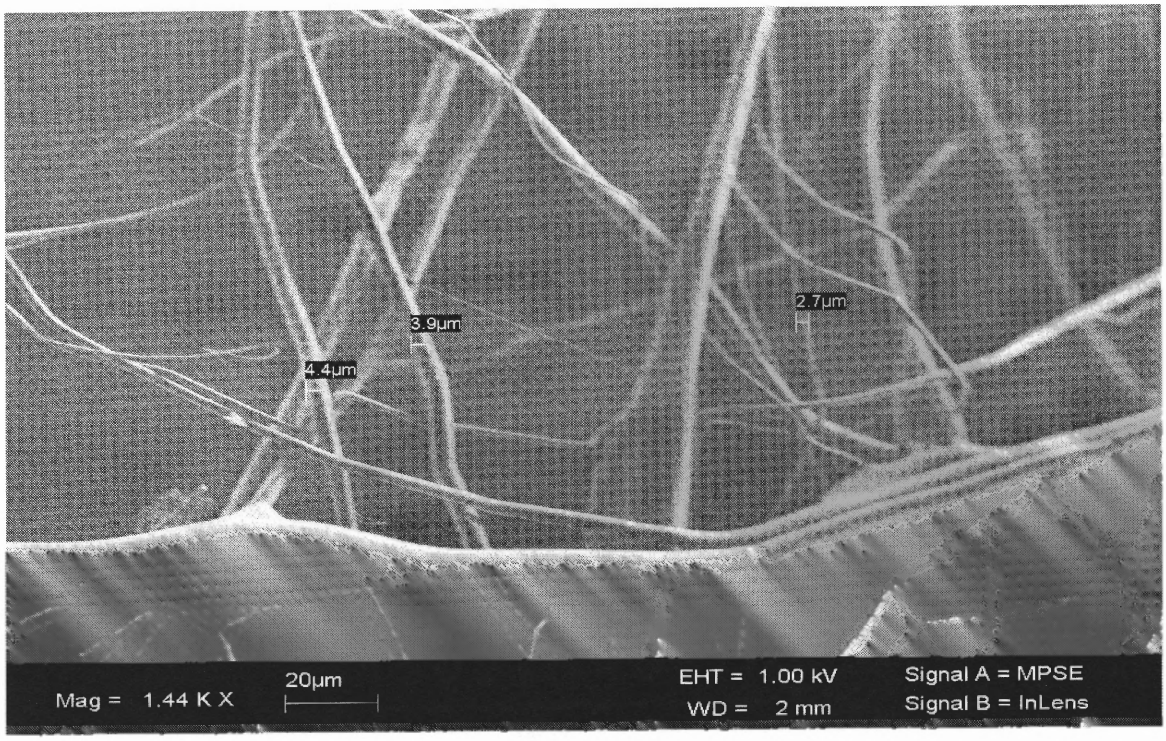

Figure 5.2 (d) 80/20-10wt% 11/25/03 20gauge.

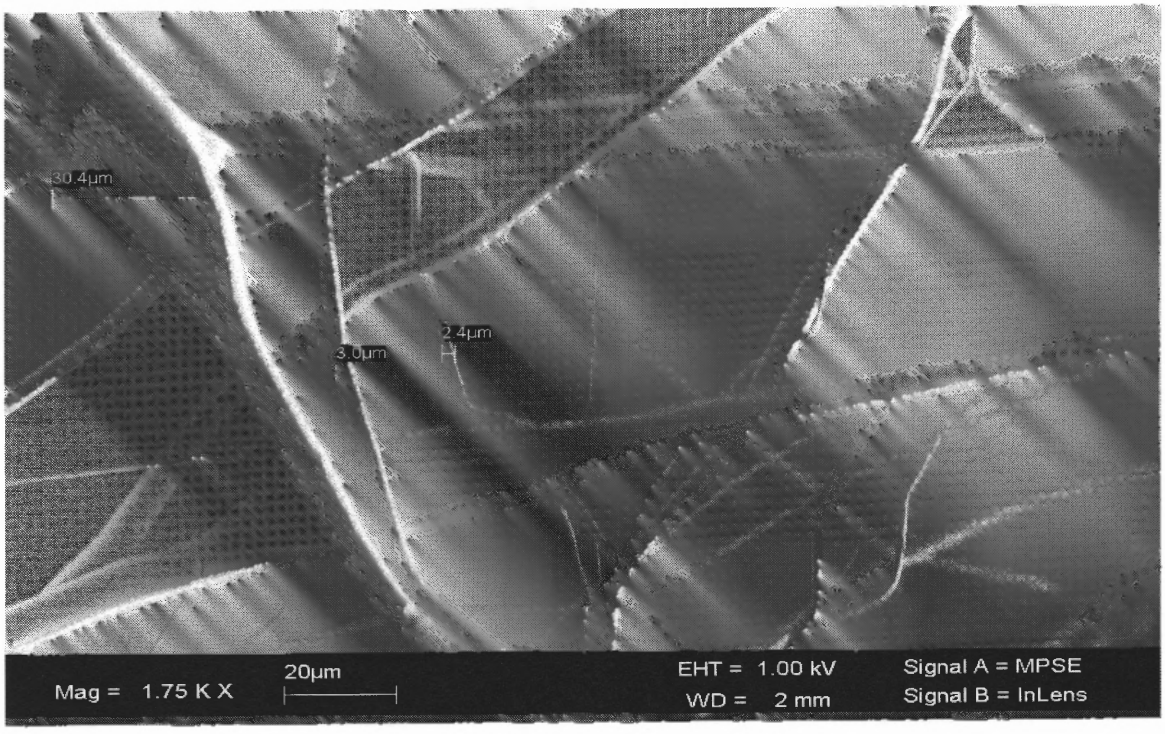

Figure 5.2 (e) 80/20-10wt% 11/25/03 20gauge.

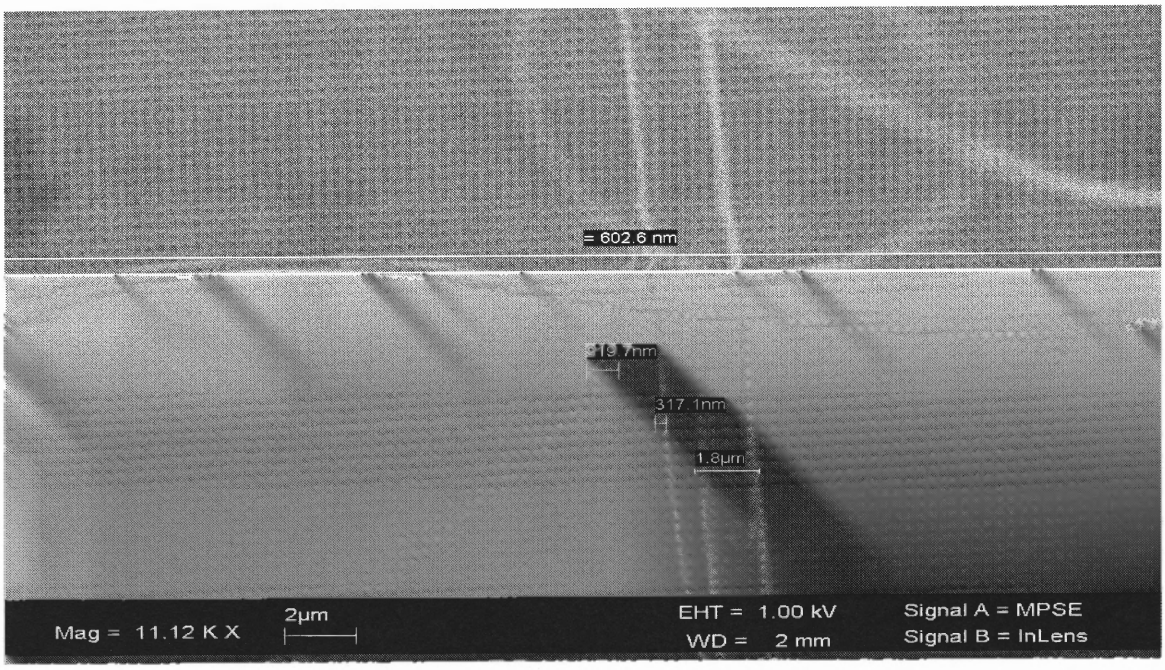

Figure 5.2 (f) 80/20-10wt% 11/25/03 20gauge.

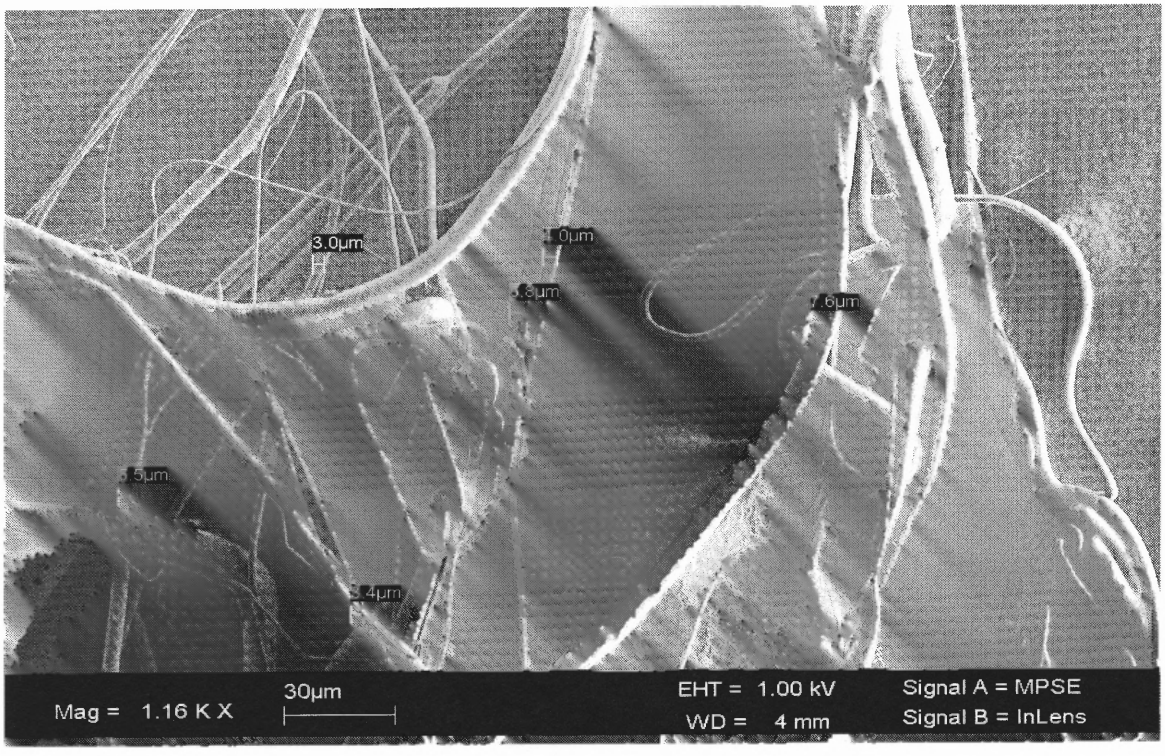

Figure 5.2 (g) 80/20-10wt% 11/25/03 22gauge.

After 11/25/03, there was more extrusion of fibers therefore a greater diameter range was noticeable. Different fiber morphologies were observed and beading was less apparent.

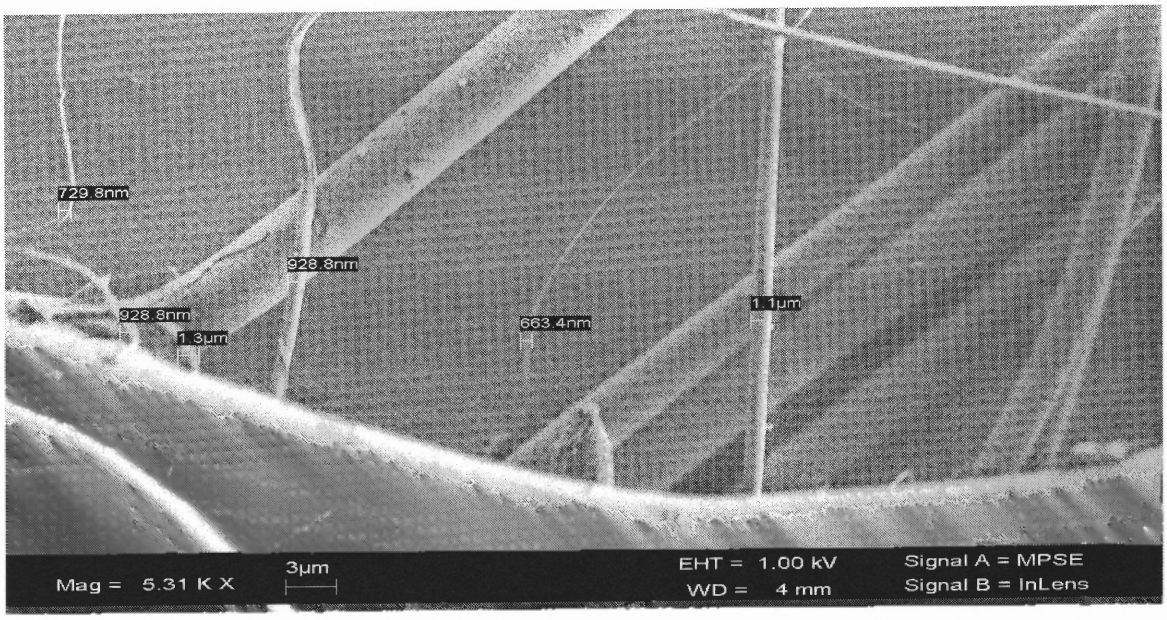

Figure 5.2 (h) 80/20-10wt% 11/25/03 22gauge.

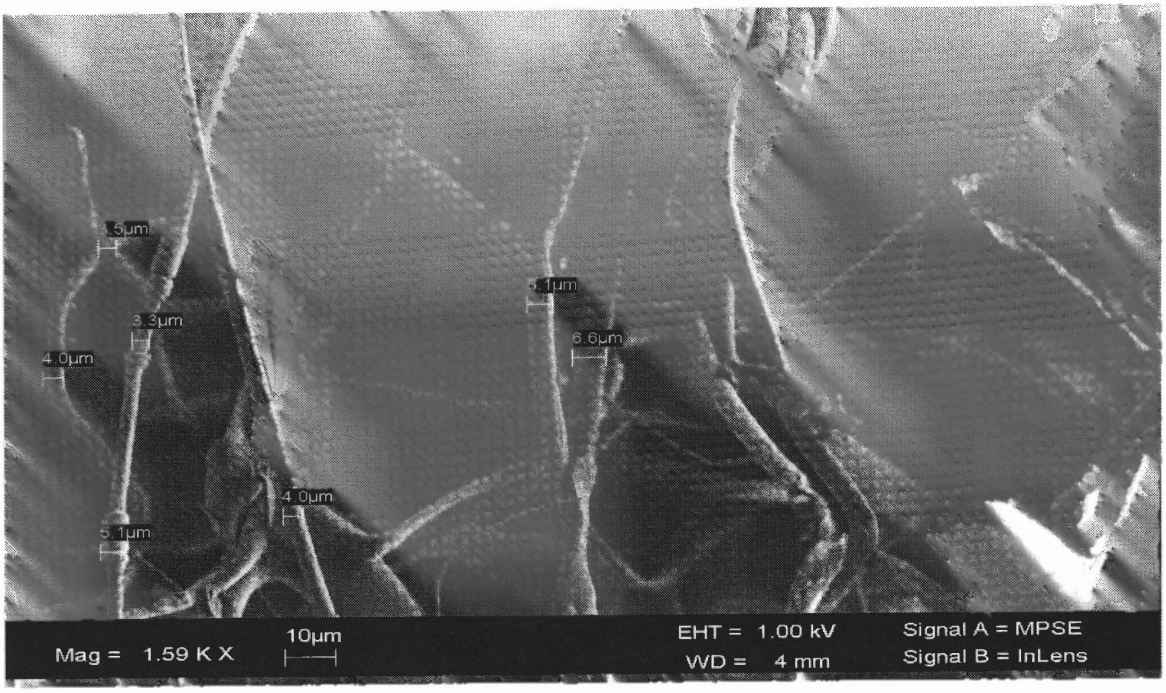

Figure 5.2 (i) 85/15-6wt% 12/01/03 22gauge.

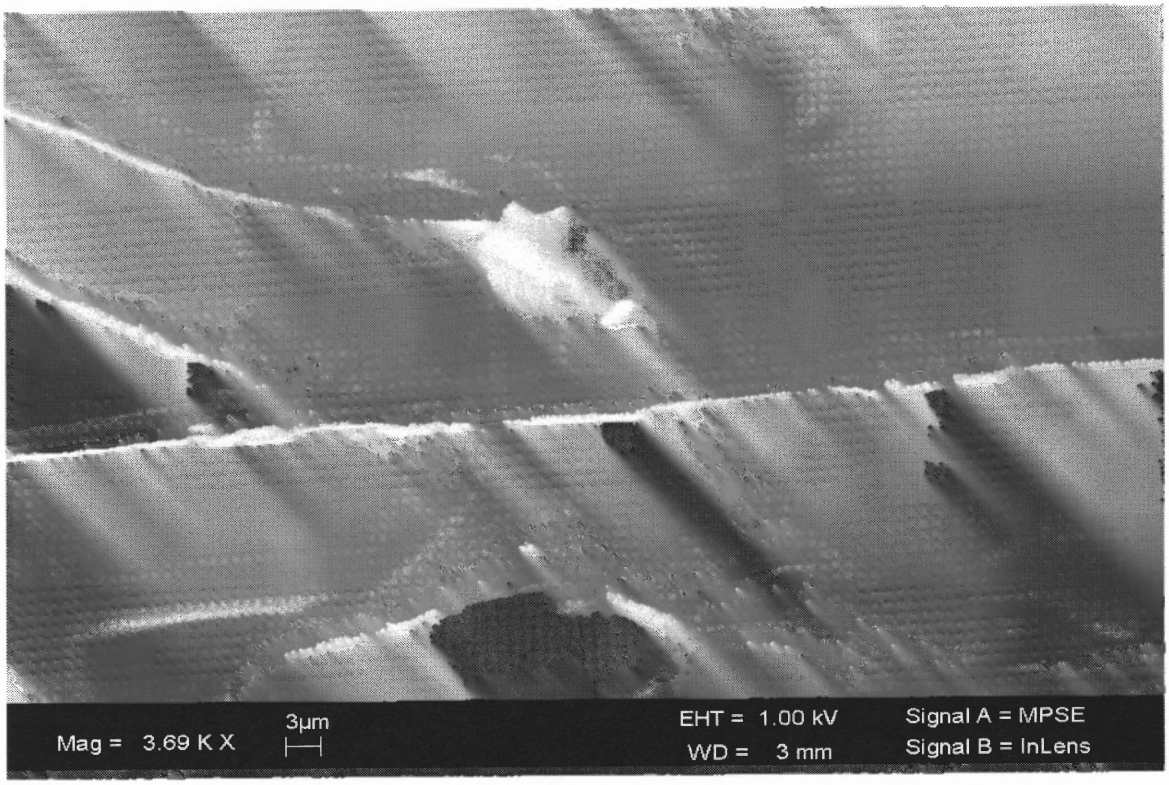

Figure 5.2 (j) 85/15-6wt% 12/01/03 22gauge.

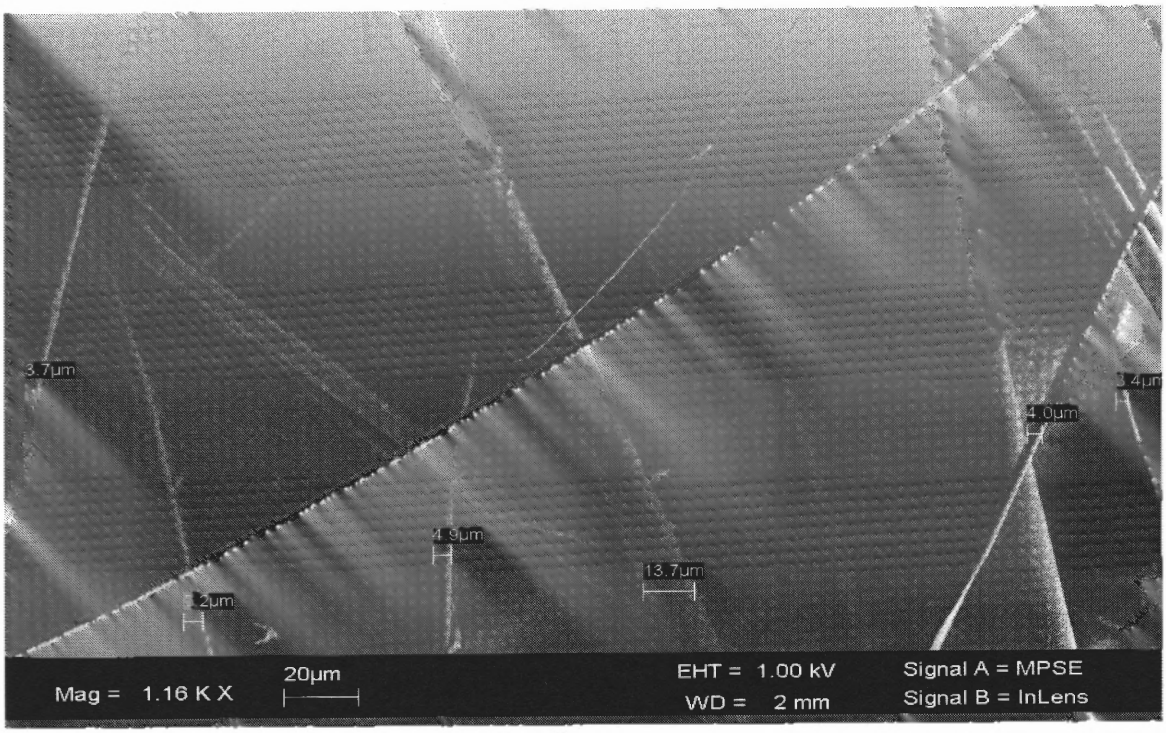

Figure 5.2 (k) 85/15-6wt% 12/01/03 20gauge.

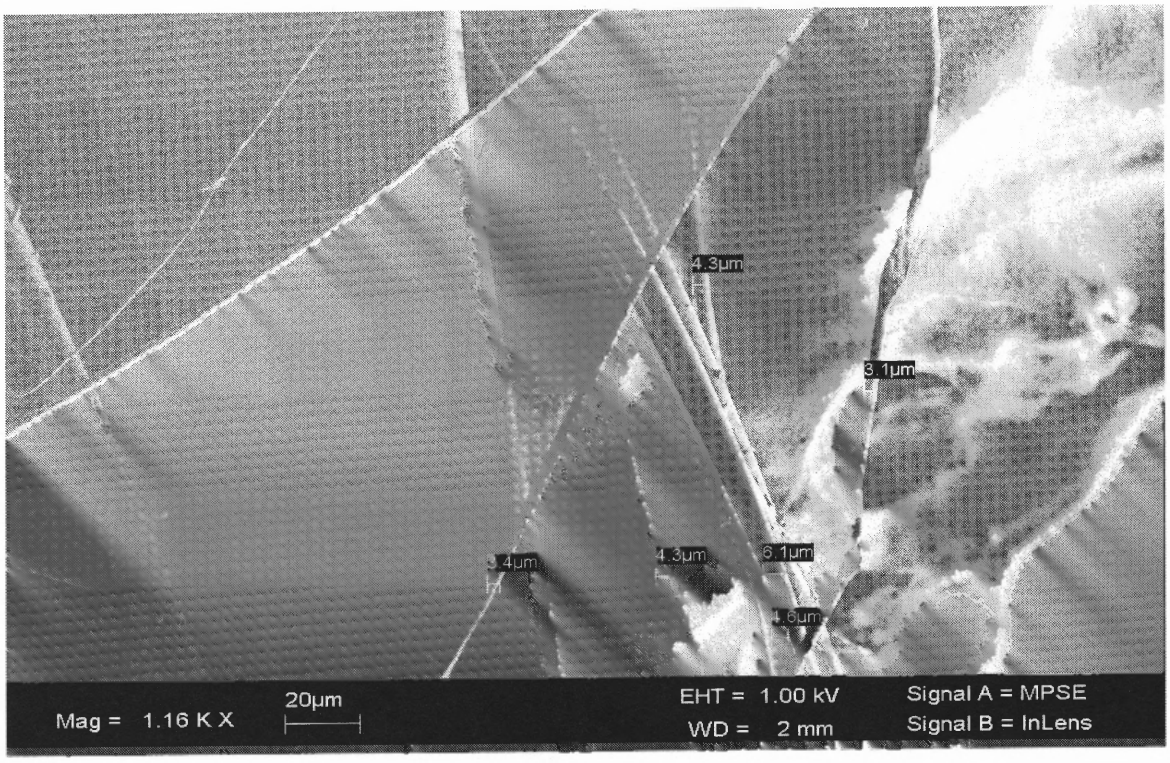

Figure 5.2 (l) 85/15-6wt% 12/01/03 20gauge

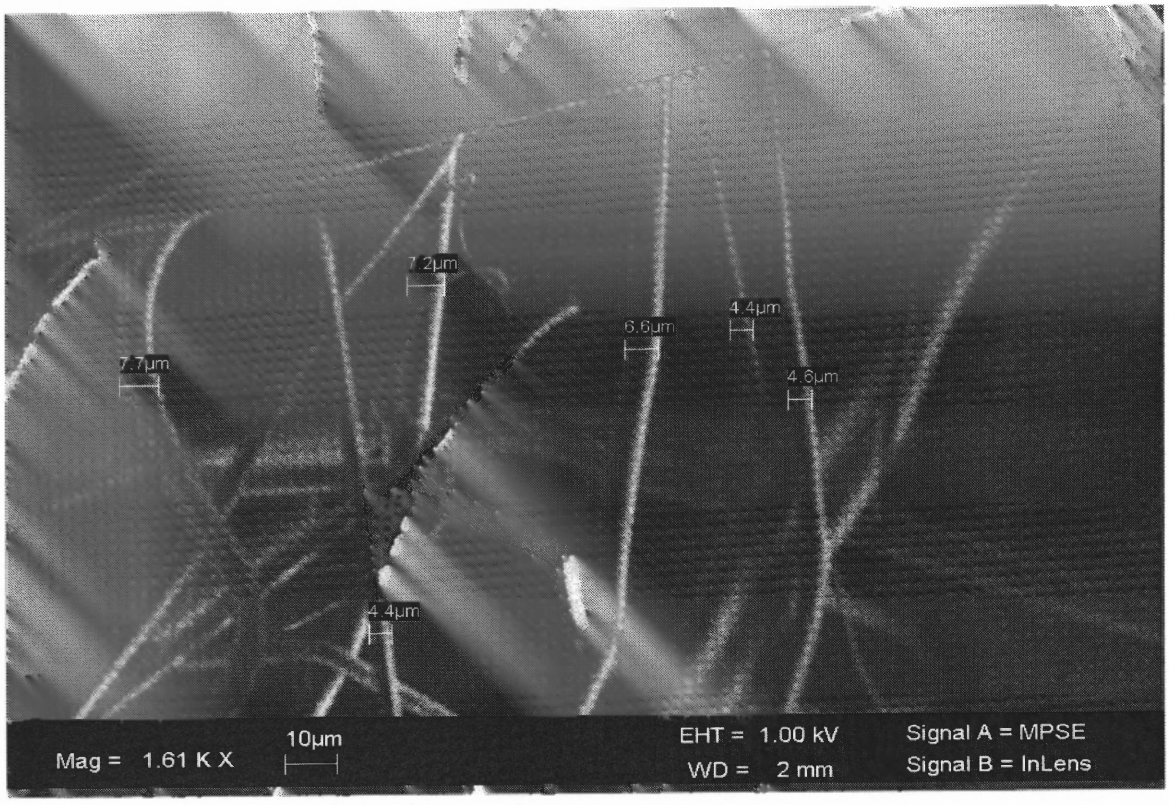

Figure 5.2 (m) 85/15-10wt% 12/04/03 22gauge.

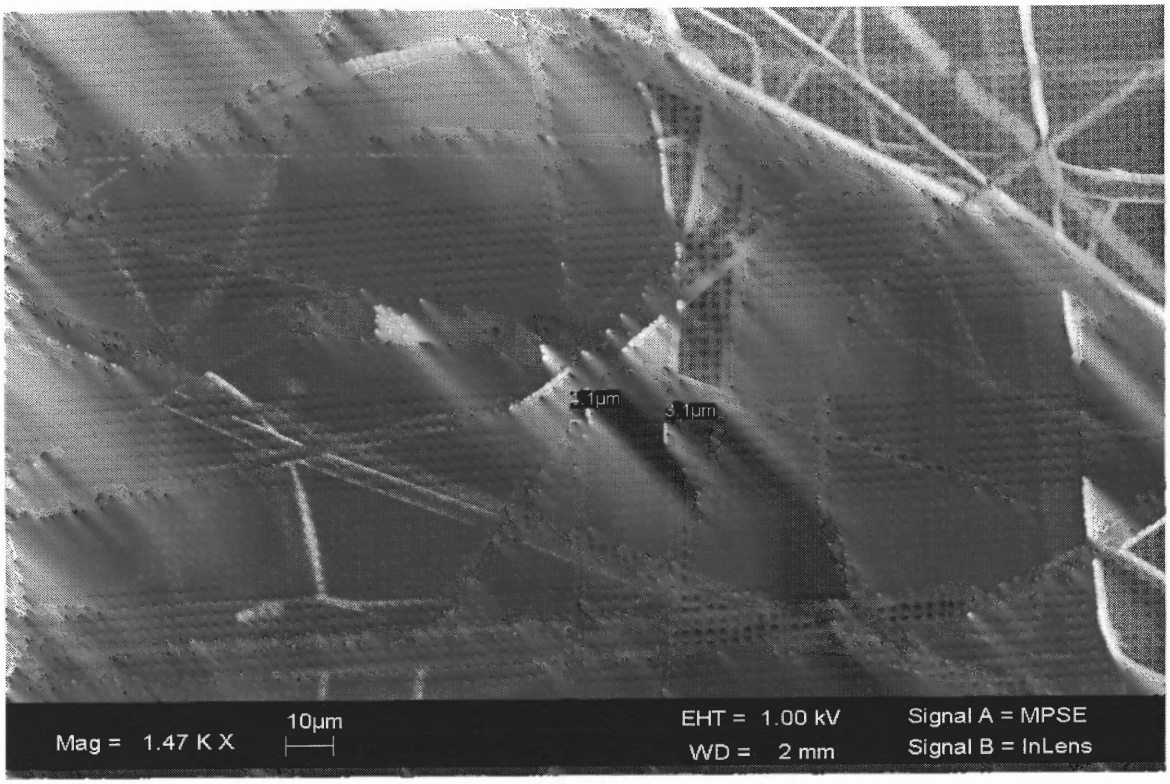

Figure 5.2 (n) 85/15-10wt% 12/04/03 22gauge.

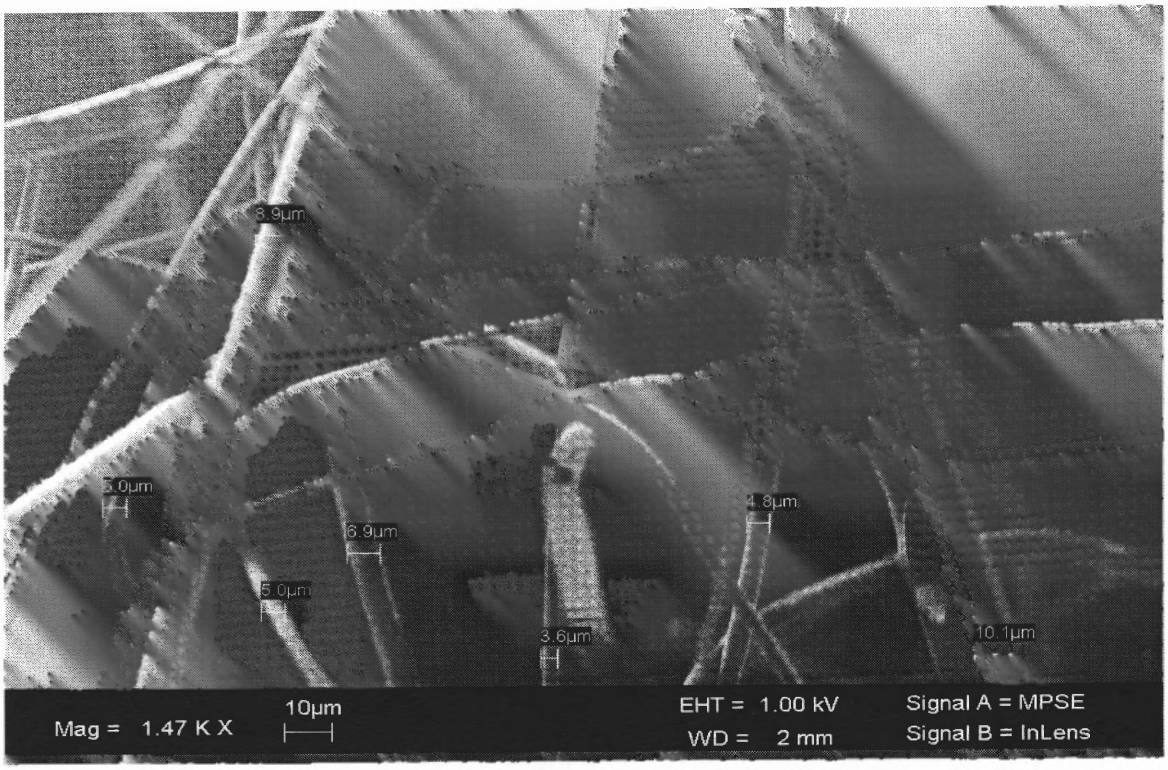

Figure 5.2 (o) 85/15-10wt% 12/04/03 22gauge.

Figure 5.2 (p) and (q) are representations of the glove sample. The latex glove was used as a collection surface for all fibers of different wt% and ratios, during the electrospinning process. The fibers have a porous morphology, due to the evaporation of solvent from the surface (increasing pore size).

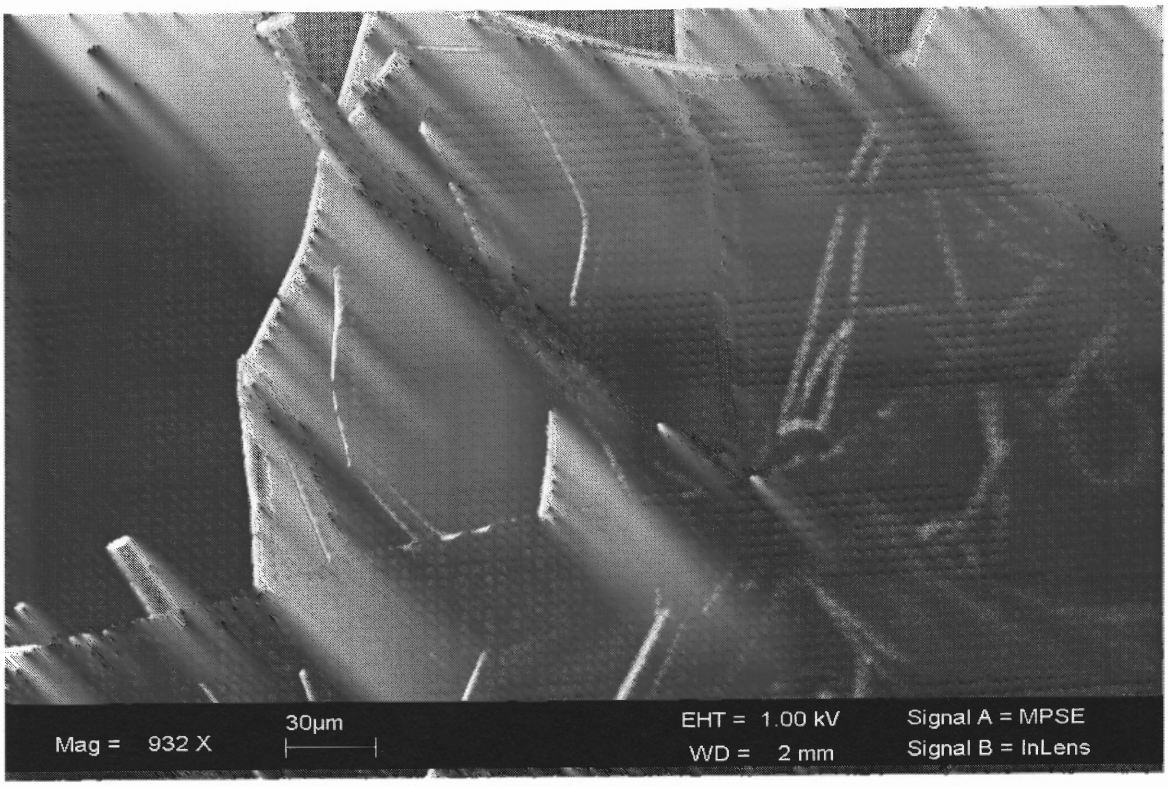

Figure 5.2 (p) glove sample-multi 11/15/03.

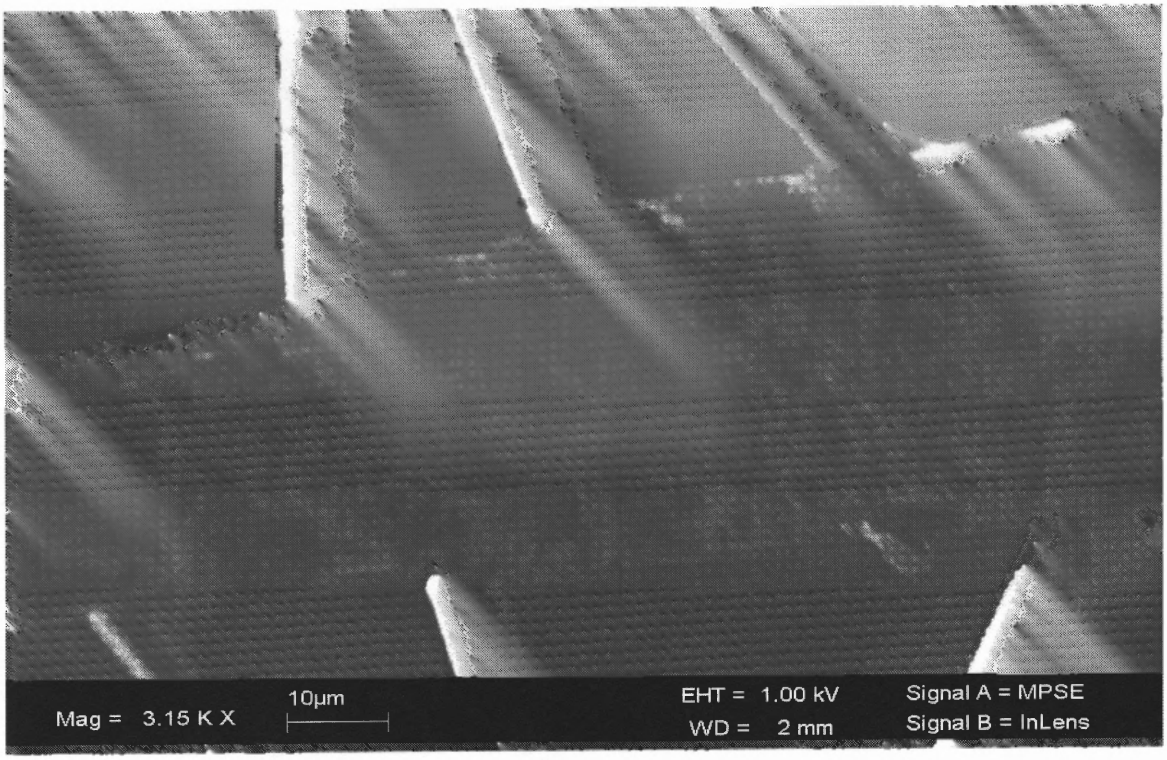

Figure 5.2 (q) glove sample-multi 11/15/03.

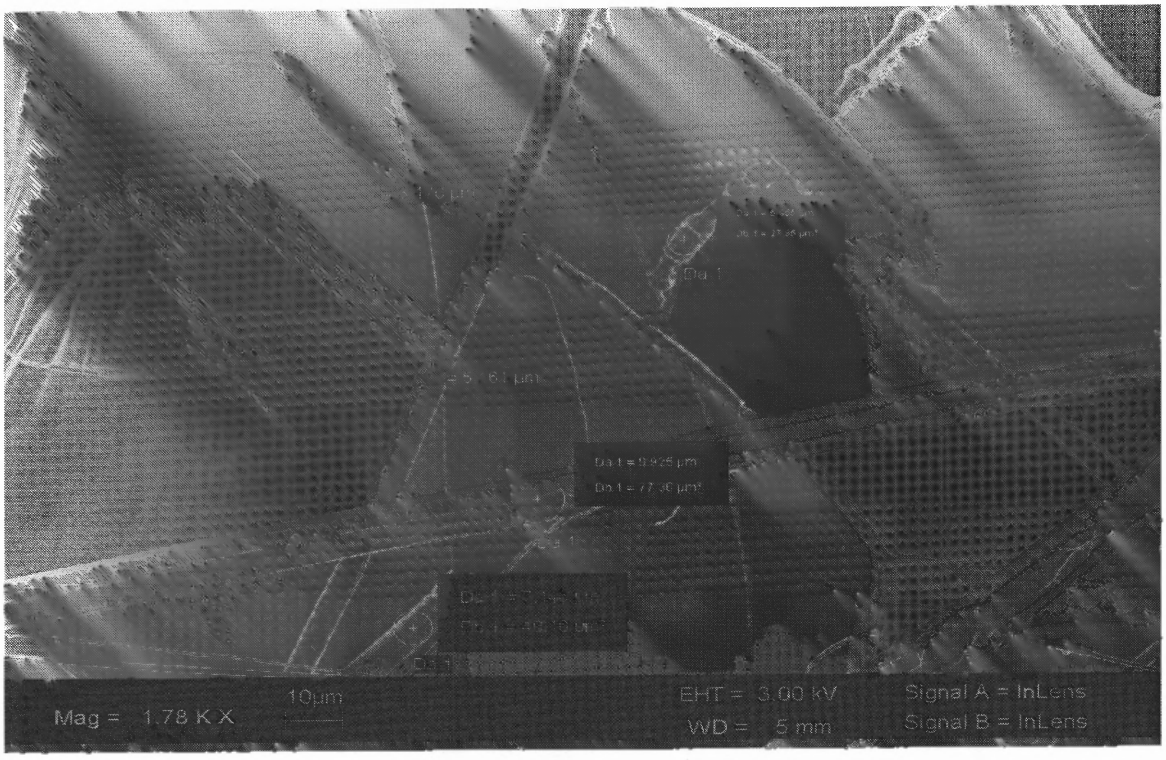

Figure 5.2 (r) 85/15-15wt% 12/17/03 22gauge.

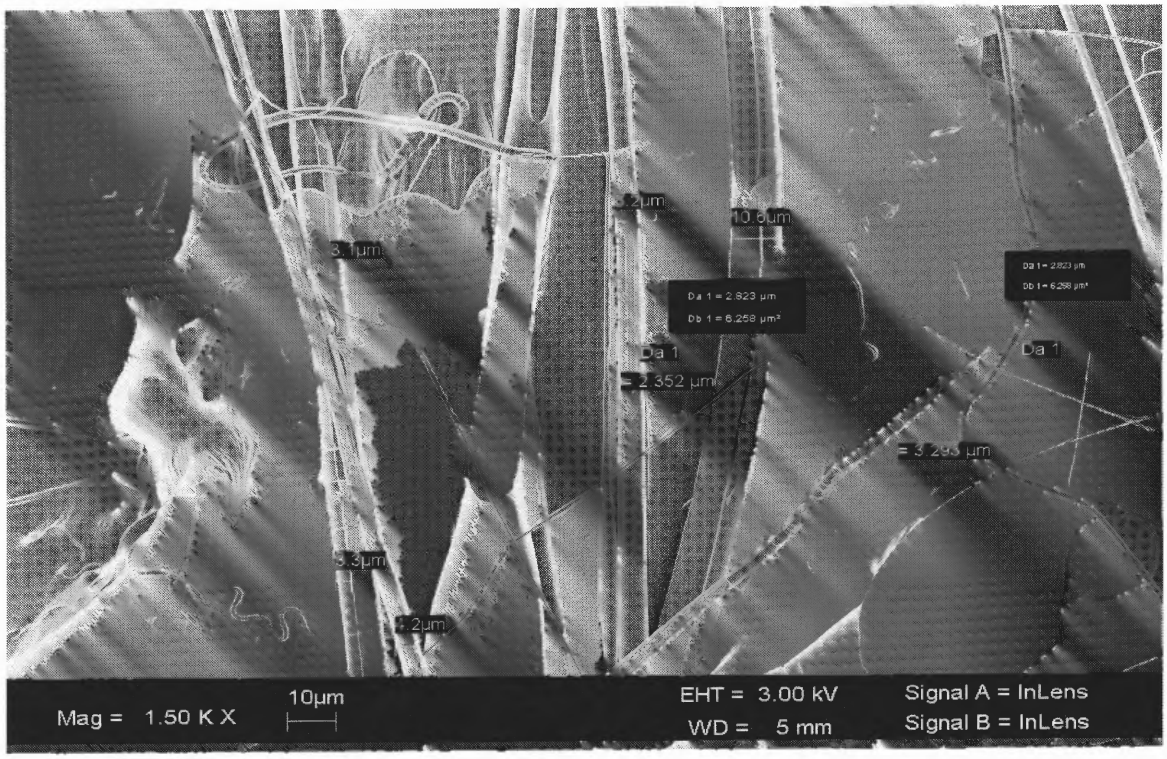

Figure 5.2 (s) 85/15-15wt% 12/17/03 22gauge.

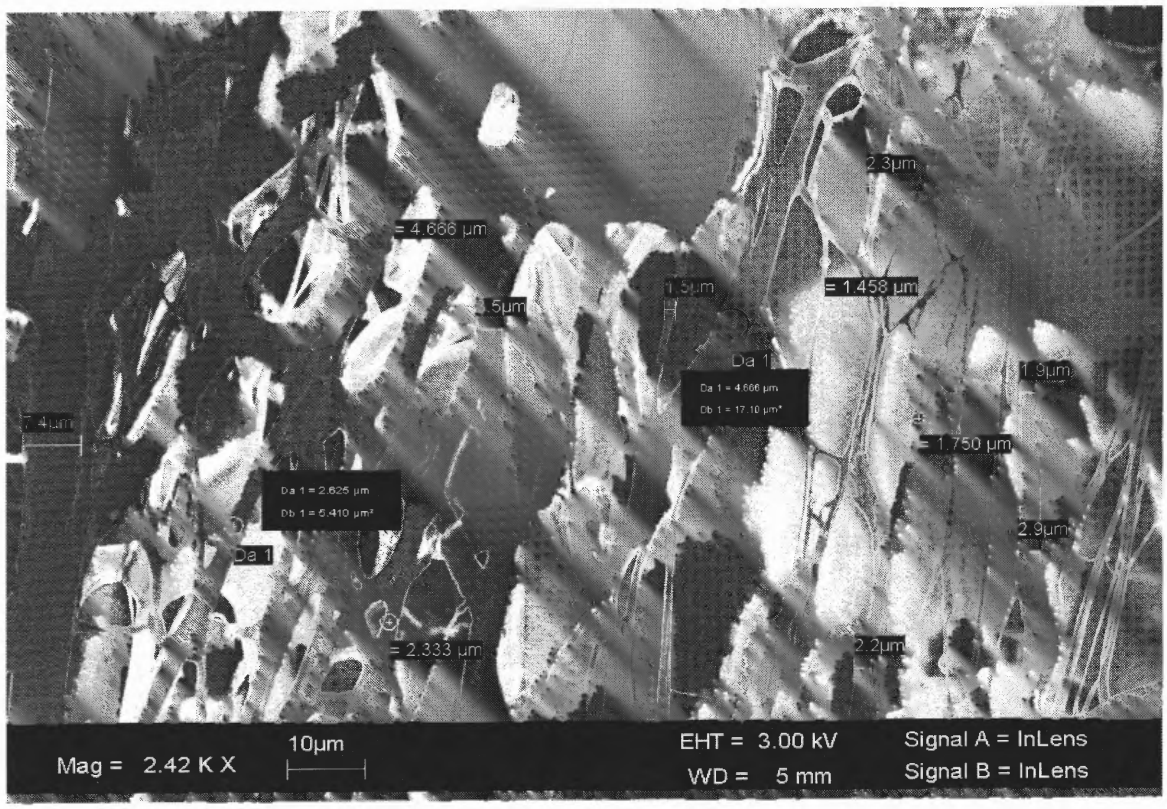

Figure 5.2 (t) 80/20-10wt% + BCNU 12/18/03 22gauge.

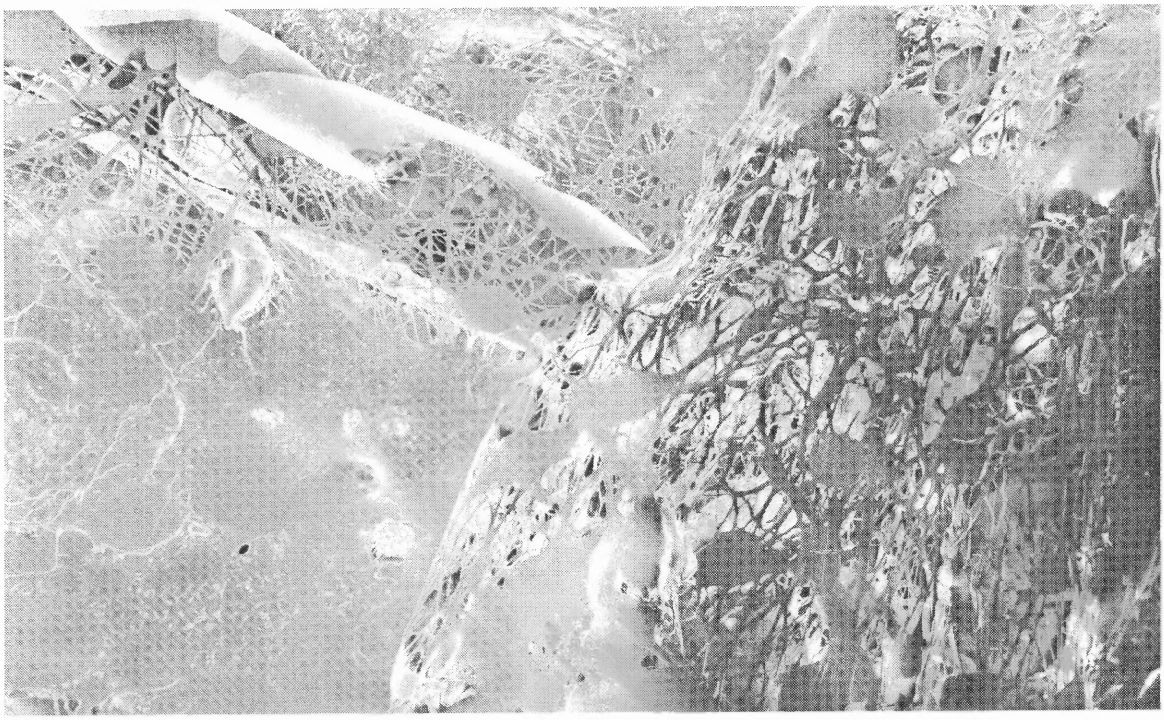

Figure 5.2 (u) 80/20-10wt% + BCNU 12/18/03 22gauge.

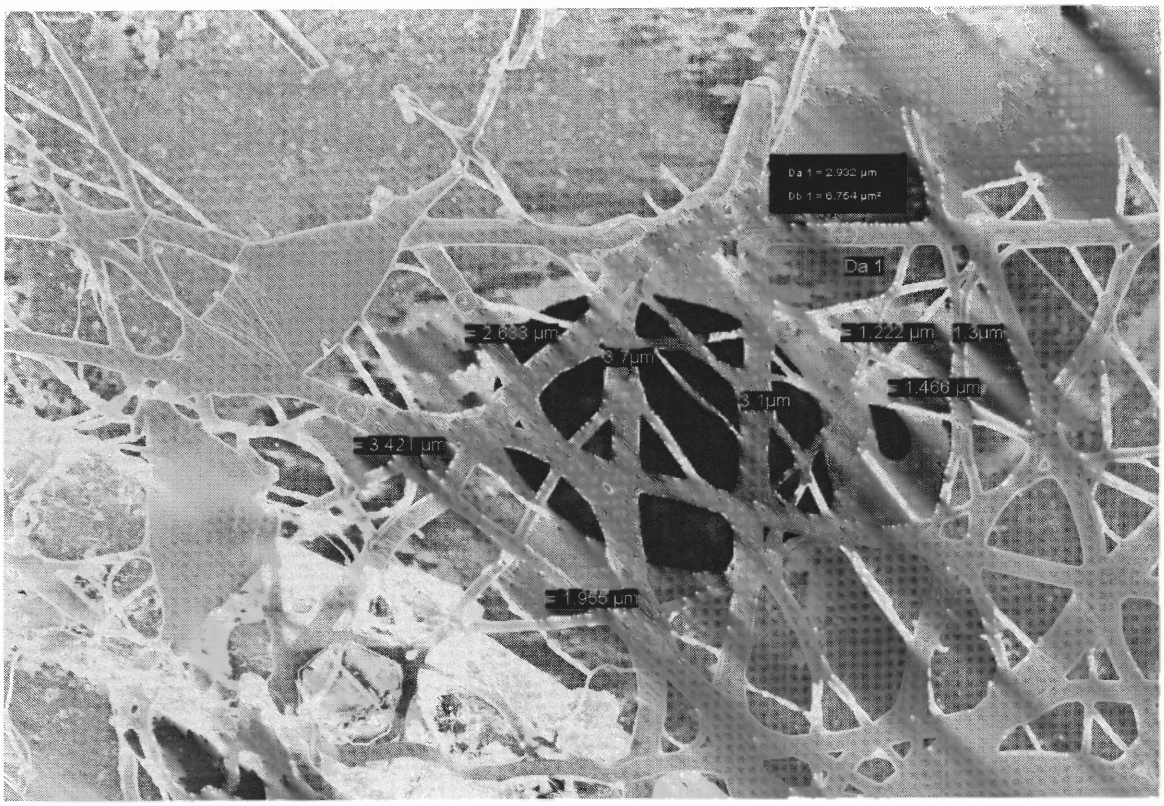

Figure 5.2 (v) 80/20-10wt% + BCNU 12/18/03 22gauge.

Using SEM analysis, the following fiber diameters were measured [Table 5.2]. The samples were also tagged by date to track the settling of the polymers in solution. The average diameter was obtained by totaling the diameter measurements and dividing by the number of measurements taken.

Table 5.2 Nanofiber Diameter

Polymer sample description	Date	Diameter measured (in microns)	Average diameter (in microns)
80/20 10wt% 20gauge	11/19/03	8.3, 4.4	6.35 Min = 4.4 Max = 8.3
80/20 6wt% 22gauge	11/20/03	1.4, 0.4082, 0.2253, 0.7422, 1.4, 0.1177, 0.2746	0.684 Min = 0.1177 Max = 4.4
80/20 10wt% 20gauge	11/25/03	4.4, 3.9, 2.7, 3.0, 2.4, 0.6026, 0.9197, 0.3171, 1.8	2.23 Min = 0.3171 Max = 4.4
80/20 10wt% 22gauge	11/25/03	5.5, 3.4, 3.0, 5.8, 4.0, 7.6, 0.7298, 0.9288, 1.3, 0.9288, 0.6634, 1.1	2.91 Min = 0.6634 Max = 5.8
85/15 6wt% 22gauge	12/01/03	4.0, 3.5, 4.0, 5.1, 6.5, 5.1, 3.3	4.5 Min = 3.3 Max = 6.5
85/15 6wt% 20gauge	12/01/03	3.7, 5.2, 4.9, 4.0, 3.4, 3.4, 4.3, 4.3, 6.1, 4.6, 3.1	4.27 Min = 3.1 Max = 6.1
85/15 10wt% 22gauge	12/04/03	7.7, 4.4, 7.2, 6.6, 4.4, 4.6, 4.1, 3.1, 5.0, 8.9, 5.0, 6.9, 3.6, 4.8, 10.1	5.76 Min = 3.1 Max = 10.1

From Table 5.2, the 80/20-10wt% and the 85/15-6wt% produced the best fibers without considering time as a factor. With time a factor in the process (the amount of time it takes for the polymer solution to settle in order to produce small diameter fibers), a sample of 80/20-8wt% and an 85/15-15wt% was made. The samples were electrospun and observed under the OM [Table 5.3].

Table 5.3 OM Fiber Observations

Date	Polymer	Wt%	Needle size	Description
12/09/03	80/20	8wt%	22gauge	Droplets
12/09/03	85/15	15wt%	22gauge	Droplets
12/15/03	80/20	8wt%	22gauge	Droplets, encapsulation
12/15/03	85/15	15wt%	22gauge	Fibers and beading
12/17/03	80/20	8wt%	22gauge	Droplets and multiple fibers
12/17/03	85/15	15wt%	22gauge	Good fiber formation, droplets, gel-like fibers
12/18/03	80/20	8wt%	22gauge	Fibers with uniform diameter, droplets, gel-like
12/18/03	85/15	15wt%	22gauge	Fibers and droplets

Gel-like fibers look like fibers in an unstable form. They have definite shape, but look as if the walls of the fiber could collapse and gel-like substance (high viscosity) would pour out. Encapsulation is when the beads of the fiber seem to show a three-dimensional image within the bead itself, by encapsulating the un-settled polymer or solution. The 85/15-15wt% gave the most concrete fiber formation in a non-woven sheet, and SEM analysis was conducted to find the average fiber diameter [Table 5.4].

Table 5.4 85/15-15wt% Recorded Diameter

Polymer sample description	Date	Diameter measured (in microns)	Average diameter (in microns)
85/15 15wt% 22gauge	12/17/03	5.955, 3.176, 5.161, 9.925, 7.146, 3.1, 5.2, 2.352, 10.6, 2.823, 2.823, 3.293, 4.2, 3.3	4.933 Min = 2.352 Max = 10.6

From the analysis of all the fiber diameters (average, min and max), the fiber formation, the 80/20-10wt% mixture was combined with the drug. An 85/15-6wt% plus BCNU was made, but no results (no fiber formation) were obtained. Using SEM analysis on the 80/20 10wt% plus BCNU, the following diameters [Table 5.5] were measured and an average diameter of 2.771 microns was calculated.

Table 5.5 Measured Diameter of 80/20-10wt% + BCNU

Polymer sample description	Date	Diameter measured (in microns)	Average diameter (in microns)
80/20 10wt% 22gauge	12/18/03	7.4, 4.666, 3.5, 2.625, 2.333, 1.5, 4.666, 2.3, 1.458, 1.9, 1.750, 2.9, 2.2, 3.421, 2.658, 3.7, 1.955, 3.1, 2.932, 1.222, 1.3, 1.466	2.771 Min = 1.3 Max = 7.4

The morphology of the 80/20-10wt% plus BCNU system was very interesting. The design looked very similar to kelp and had an intricate three-dimensional structure [Figure 5.2 (t), (u)].

Using the TGA analysis, all samples, with and without the drug showed a mass loss of between 4-8% [Figure 5.3 (a), (b)].

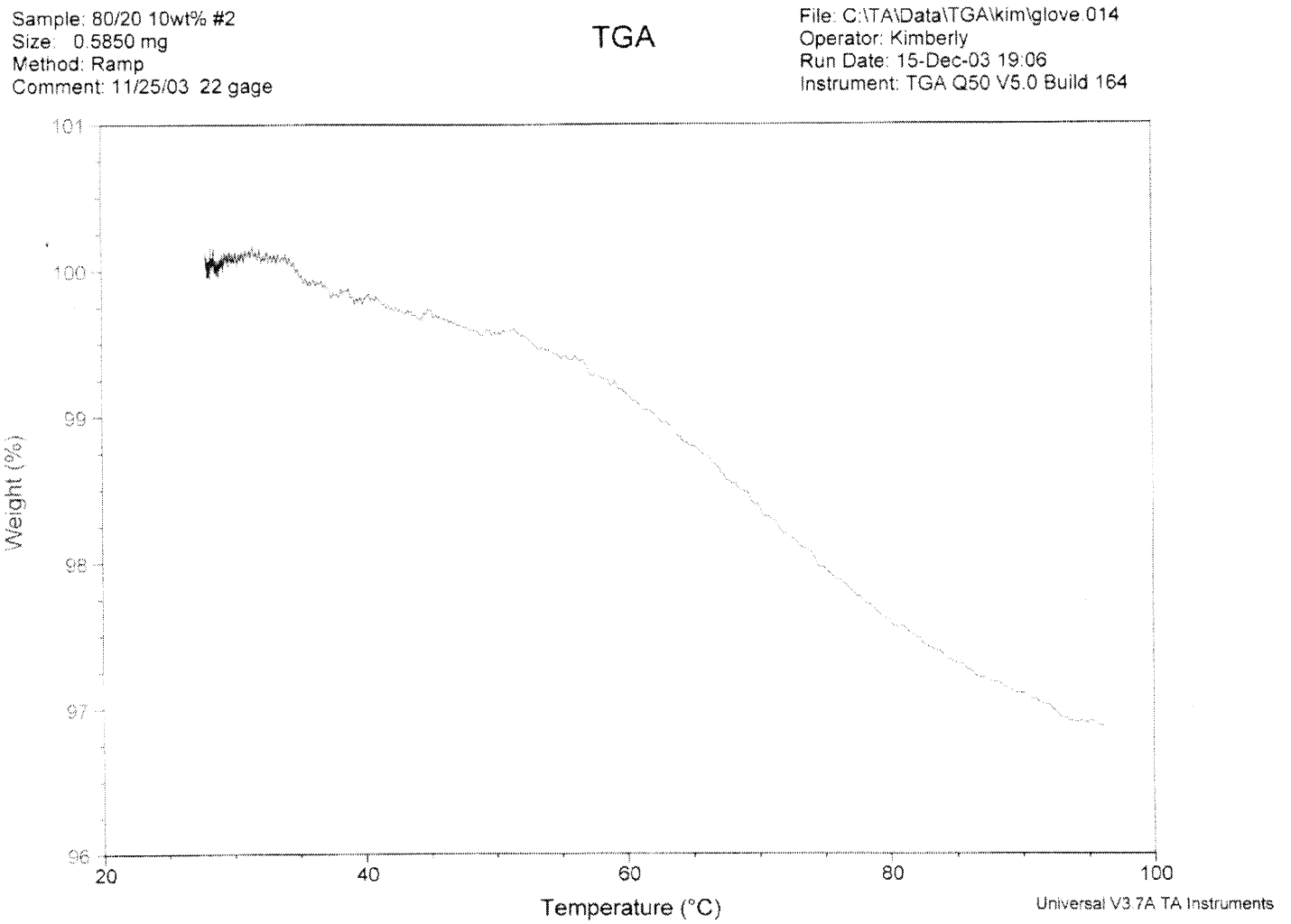

Figure 5.3 a TGA of 10% wt DLPLGA nanofiber with ~ 3% wt mass loss.

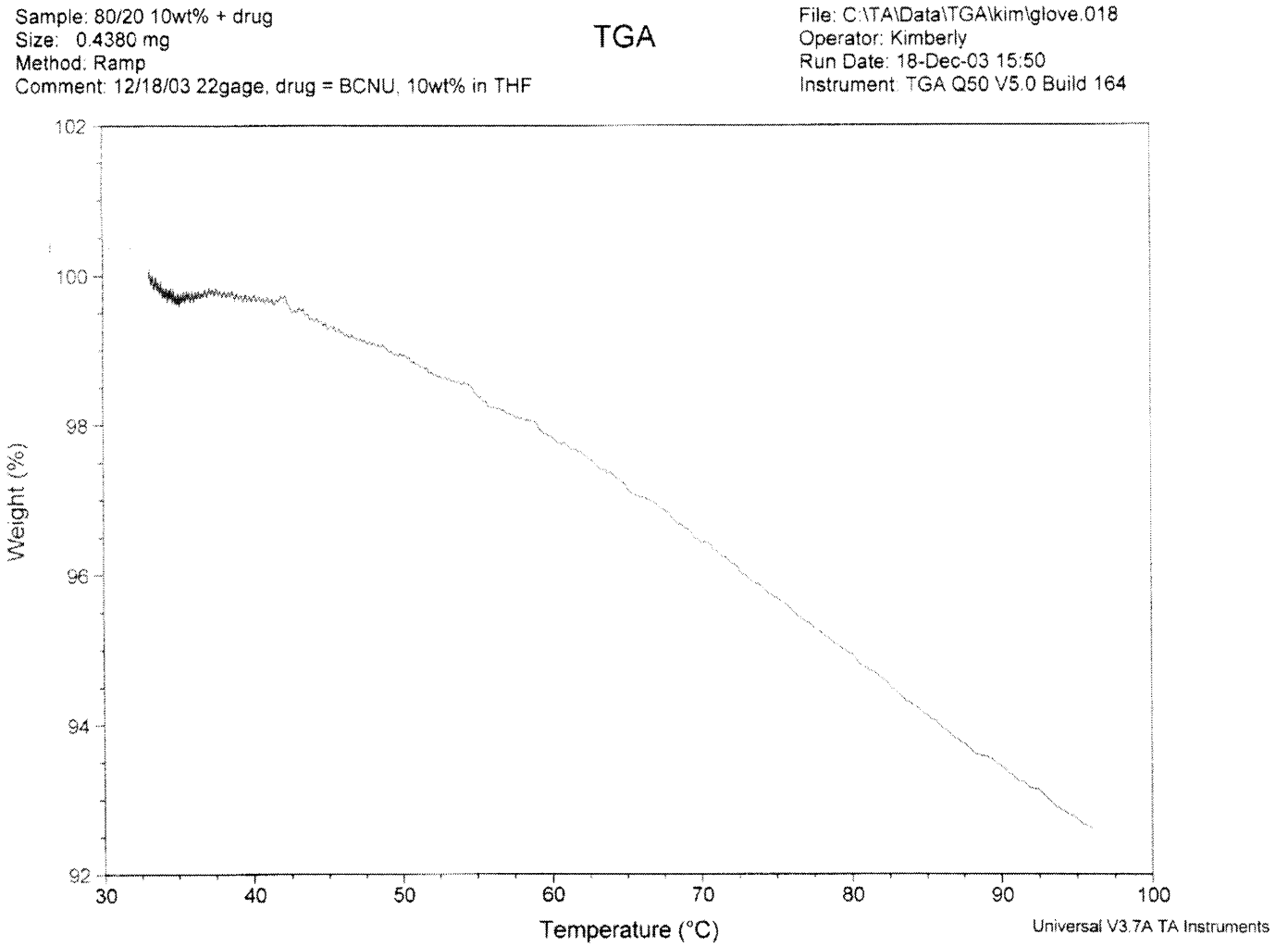

Figure 5.3 b TGA of 10% wt DLPLGA nanofiber with drug BCNU ~ 8% wt mass loss.

The DSC analysis [Figure 5.4 (a) – (d)] showed that the raw polymer and the electrospun polymer had the same Tg (glass transition temperature). A Tm (melting temperature) was not observed on the DSC graphs since the polymer is amorphous. The only change in Tg observed was subject to the presence of the drug in the polymer [Figure 5.4 (e) and (f)].

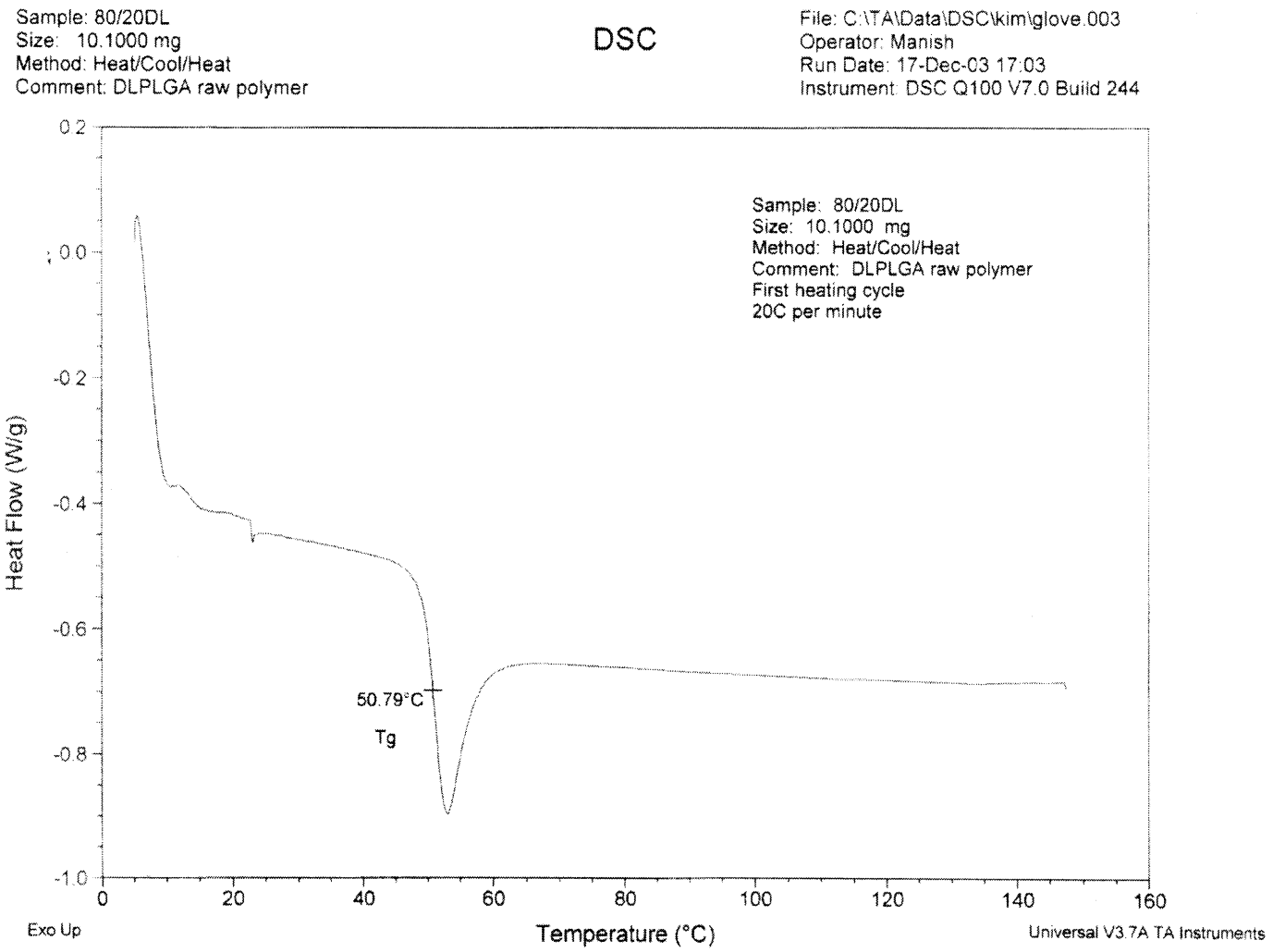

Figure 5.4 a DSC of 80/20 DLPLGA polymer , First heat cycle.

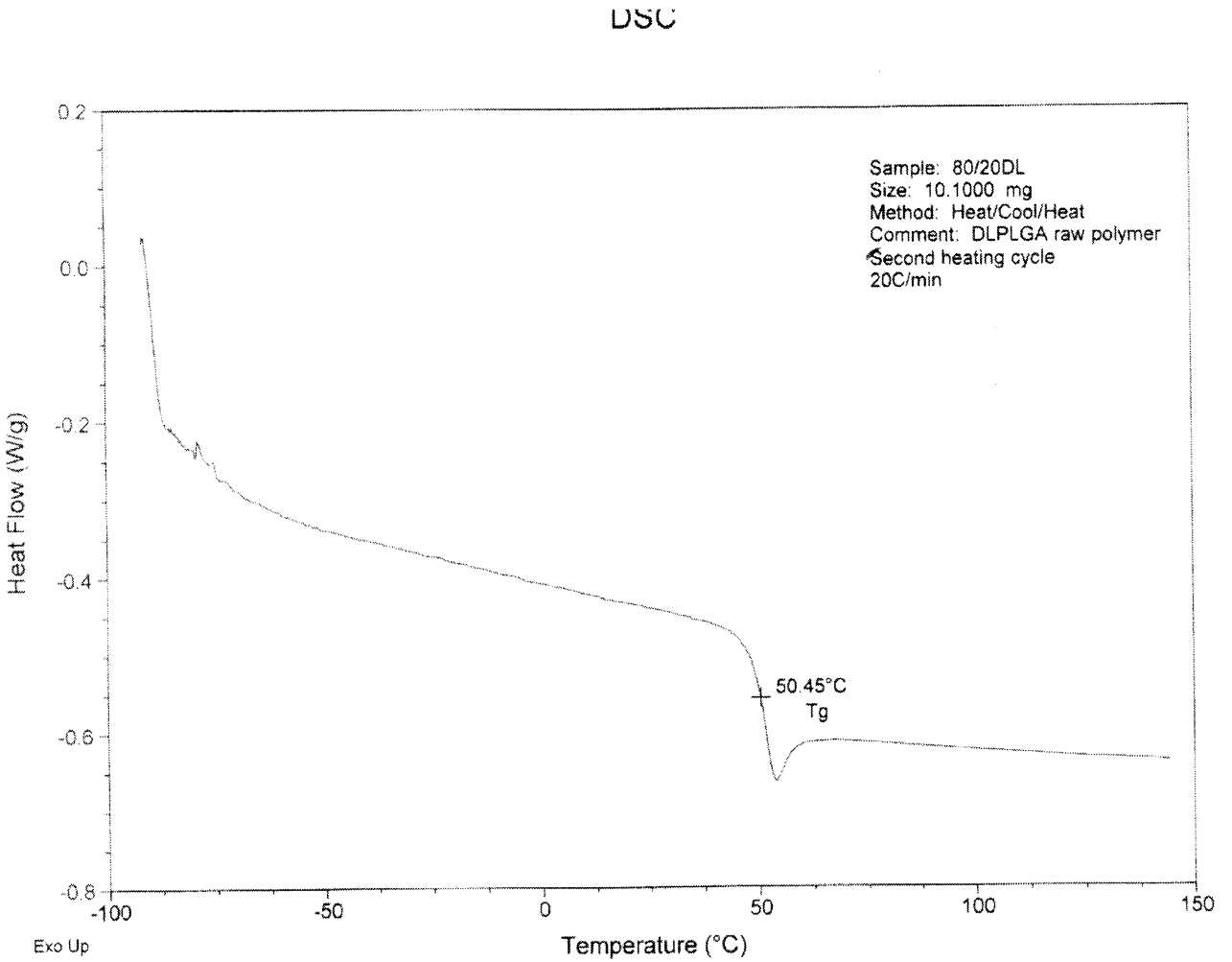

Figure 5.4 b DSC of 80/20 DLPLGA polymer , Second heat cycle.

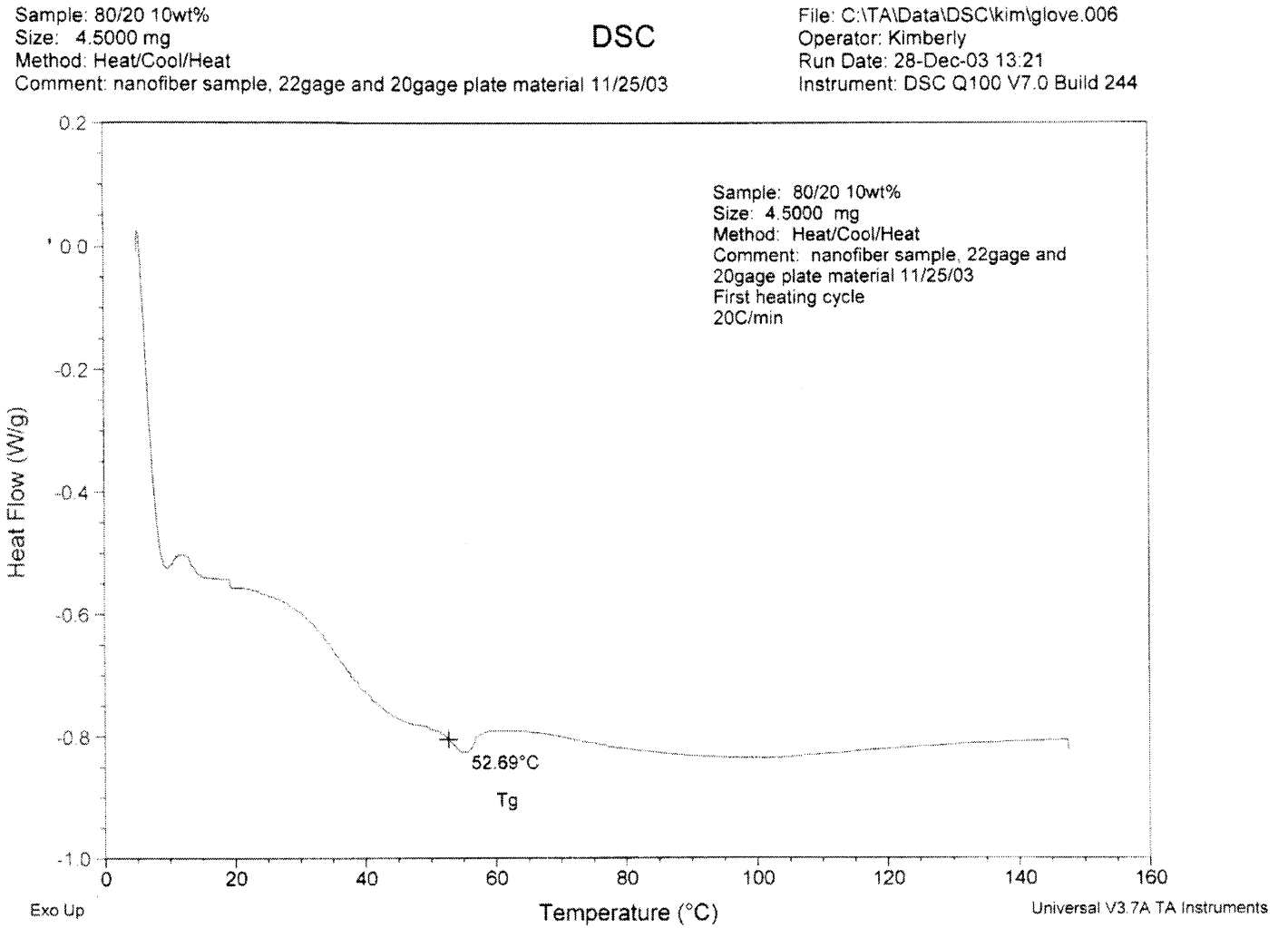

Figure 5.4 c DSC of 80/20 DLPLGA nanofiber , First heat cycle.

The DSC analysis of the nanofiber sample of 80/20-10wt% DLPLGA, second heating cycle is seen in Figure 5.4 (d). The second heating cycle could not be isolated due to computer programming errors. However, a Tg was still measured for comparison. In the second heating run of the 80/20-10wt% polymer plus drug, there it is not clear as to where the actual Tg is, since due to the first heating, the drug had been degraded. The first heating cycle gives more definitive proof of the presence of the drug, before degradation [Figure 5.4 (e) and (f)].

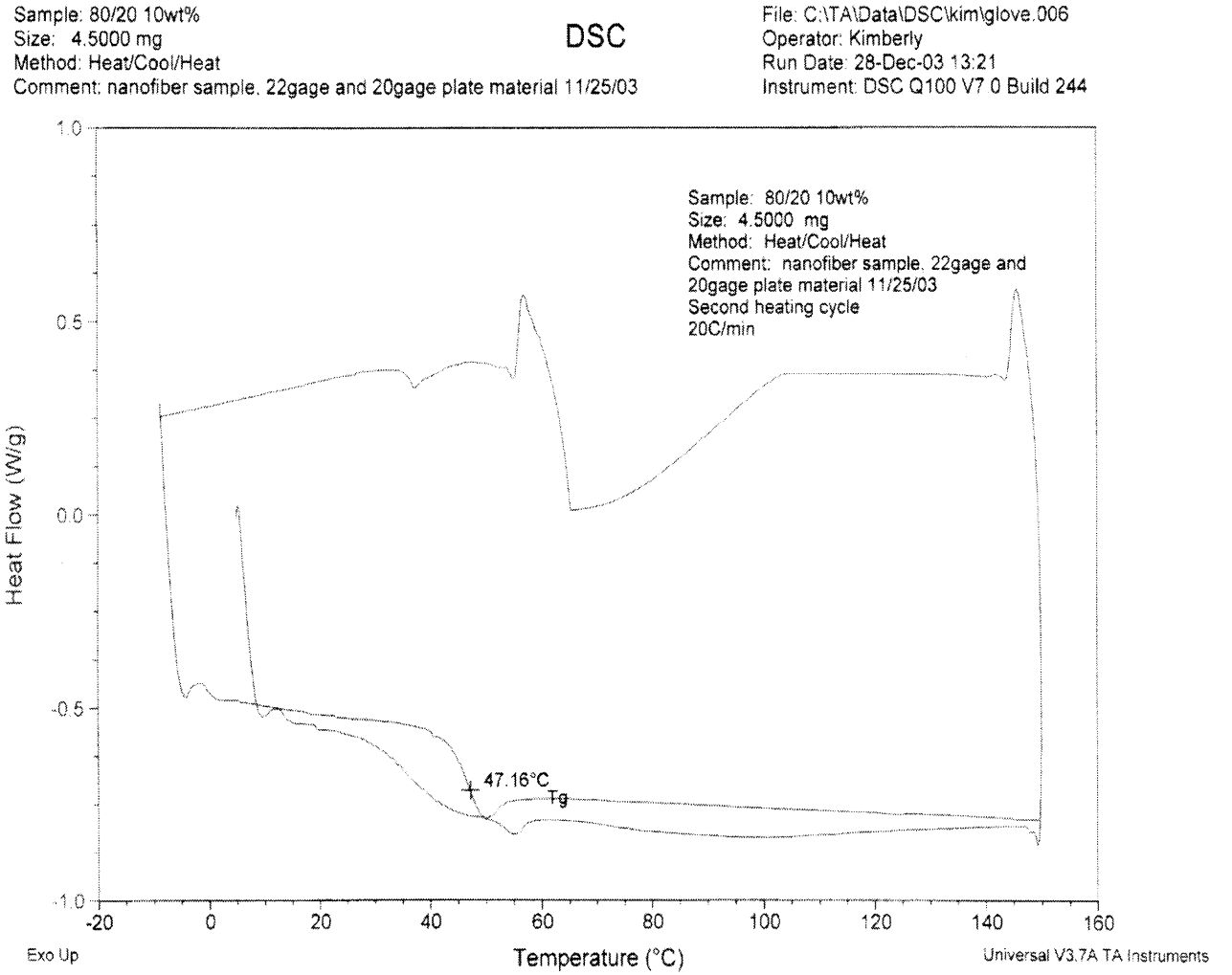

Figure 5.4 d DSC of 80/20 DLPLGA nanofiber , Second heat cycle.

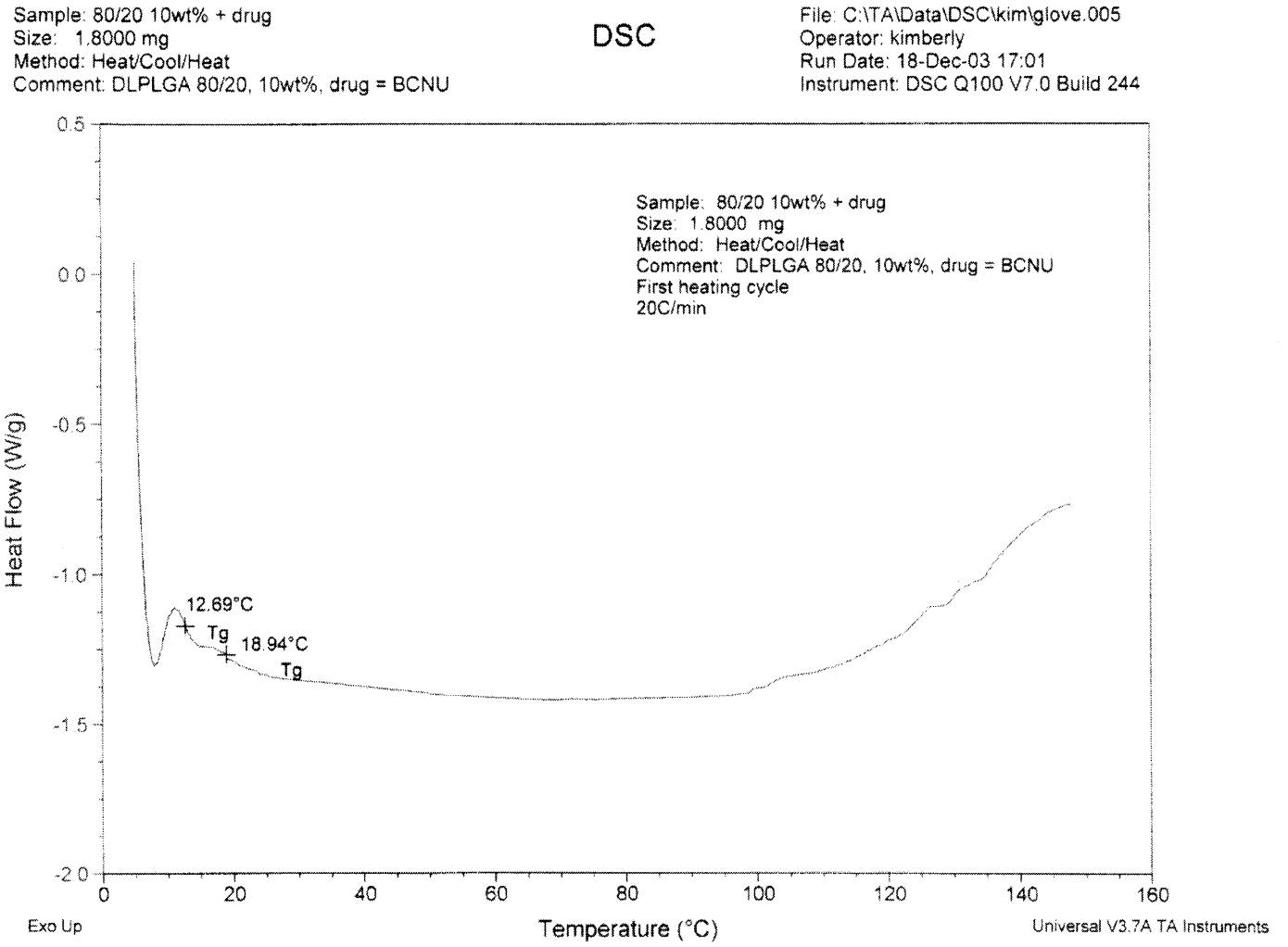

Figure 5.4 e DSC of 80/20 DLPLGA nanofiber with drug BCNU , First heat cycle.

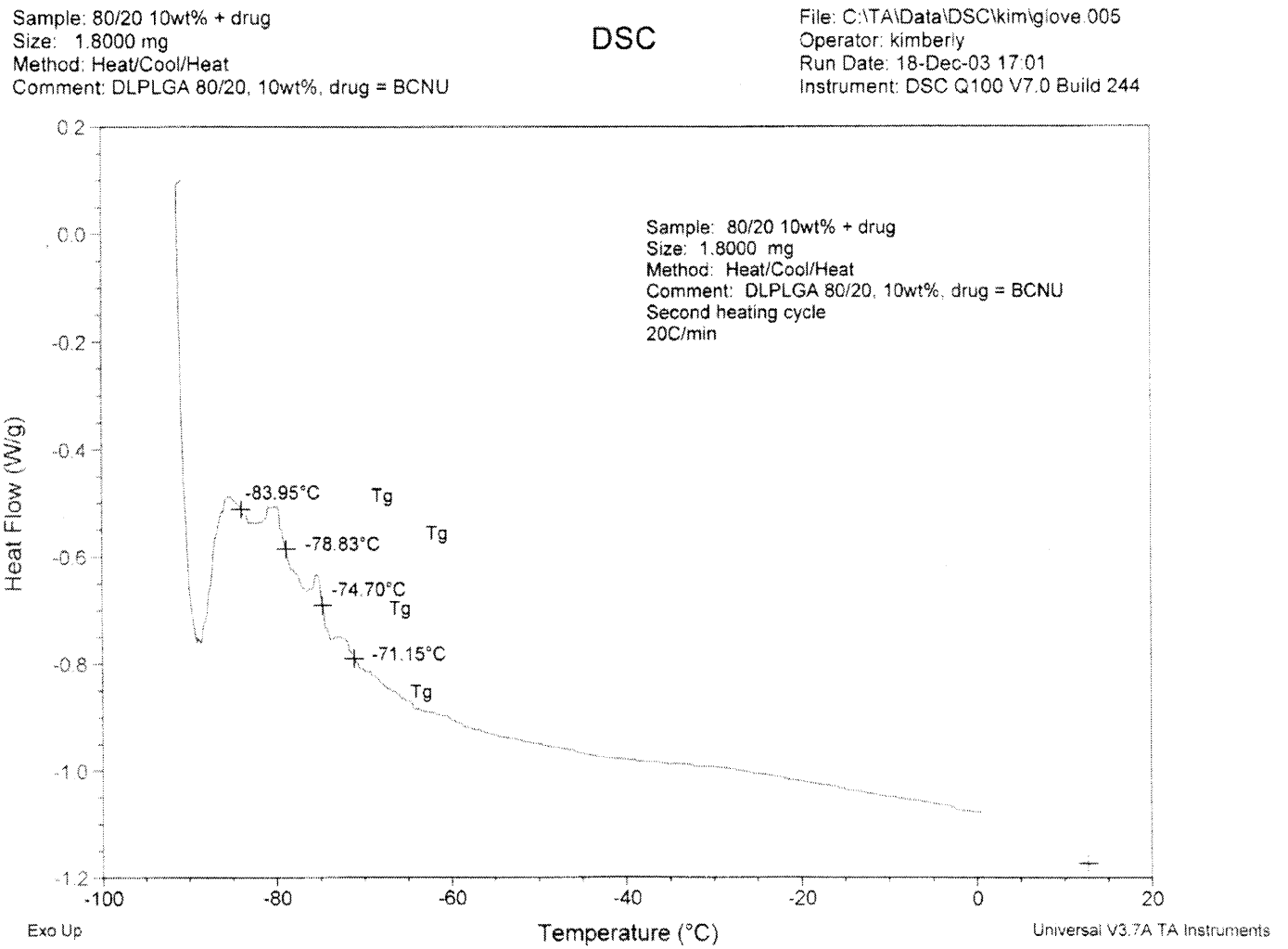

Figure 5.4 f DSC of 80/20 DLPLGA nanofiber with drug BCNU, Second heat cycle.

CHAPTER 6

DISCUSSION

A study done by the School of Biomedical Engineering, Science and Health Systems, Drexel University, PA, PLGA was electrospun in THF solvent in order to design the ideal scaffold for tissue engineering [24]. The fiber diameter range was from 500-800nanometers.

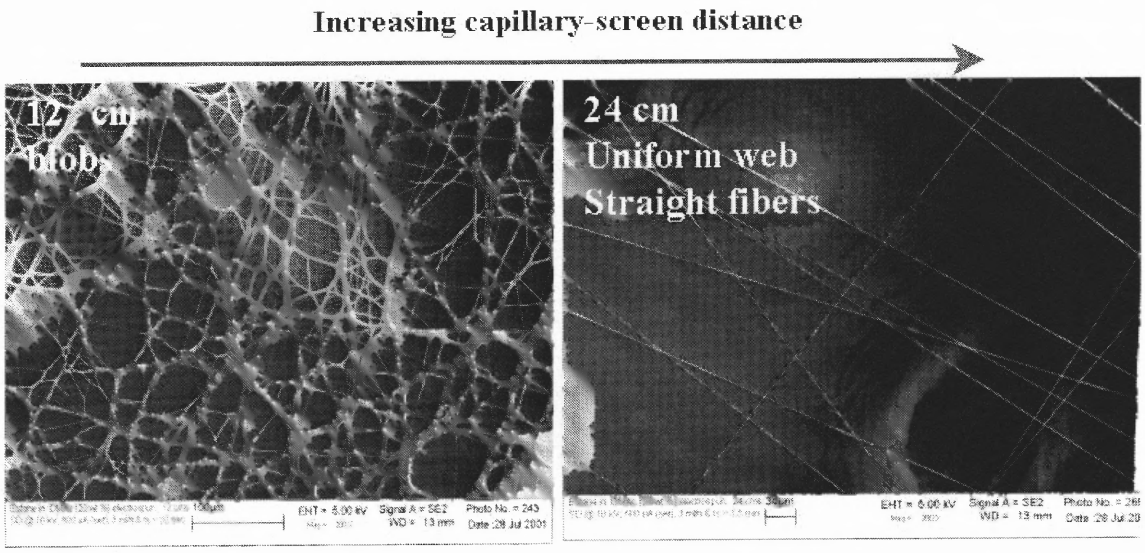

Figure 6.1 Increase distance, diameter decreases from 5um to 333nm.

The Chemical Engineering department at Virginia Tech obtained similar results, where the diameter range observed was from 5um to 333nm [Figure 6.1]. The "blobs" observed had the same morphology as the glove sample obtained in this research, where the polymer fibers seemed to have branched off of one another.

From the SEM analysis and the average diameters, no significant change in diameter was observed. An average diameter of 2.91 microns was calculated for the

80/20-10wt% alone and 2.771 microns for the 80/20 10wt% plus BCNU. The only difference observed was in the range of polymer diameter. The 80/20-10wt% alone had a min at 0.6634 microns and a max at 5.8 microns, where the 80/20-10wt% plus BCNU had a min at 1.3 microns and a max at 7.4 microns. The drug-polymer combination allowed for a wider range of polymer diameter, but not necessarily with smaller diameters (in the future, these numbers need to be repeated for consistency). While making the solution samples of 80/20-10wt%, a week was need to allow for entanglement of the polymer in order to electrospin fibers. The drug-polymer solution of the 80/20-10wt% did not need as much time to settle (entangle) and spun out fibers within a few days. The presence of the drug may have affected the critical time at which entanglement occurred and needs further investigation.

Using TGA of the plain polymer fibers (no drug) over a period of time in comparison to that with the drug combined into it, no change in solvent dissipation or mass ratio was observed. Comparing the TGA of the 80/20-10wt% and the 80/20 10wt% plus BCNU [Figure 5.3], no significant mass loss difference (difference of ~4%) was observed. In both the SEM analysis and the TGA analysis, it can be said based on the observations that the presence of the drug did not affect diameter size or amount of mass loss. Using DSC analysis, the raw polymer was compared to the plain electrospun fibers and showed no change in the Tg (glass transition temperature). This provided proof that the electrospinning process does not affect the polymer's properties.

Also, in comparing the raw polymer with the 80/20 10wt% electrospun polymers in both the TGA and DSC, the electrospinning assay did not affect the polymer characteristics. In the DSC graphs [Figure 5.4 (a)-(d)], the 80/20 10wt% and the 80/20

raw polymer graphs had the same Tg, around 48-53 °C, as was expected and reported by Appendix E. Comparing the DSC of the 80/20 10wt% plus BCNU to the 80/20-10wt% alone, there was a significant change in the Tg [Figure 5.4 (c)-(f)]. The Tg was reported at 12.69°C and 18.94°C, as is concurrent with findings found at the department of Pharmacy and Pharmaceutical Technology (Madrid Spain). This change in DSC allowed for the assumption that the drug was present in the polymer.

In a study done by the department of Pharmacy and Pharmaceutical Technology (Madrid, Spain), using BCNU encapsulated Poly (D, L-lactide-coglycolide) microspheres (ratio 0.2 - 1.5 drug/polymer ratios), the diameter of the microspheres increased and the encapsulation efficiency decreased. The BCNU content of the microspheres decreased TG onset of the polymer [23]. As an extended beneficial characteristic, the electrospun drug delivery system releases high concentrations of the drug in small dosage forms to the target site, therefore decreasing the side effects and/or toxicities that are possible when administering BCNU. With skin contact of the drug in the electrospun fiber, an allergic reaction occurred, leading to the hypothesis that the nanofibers can support the drug functionality much longer than in other physical or chemical forms such as I.V. Further analysis on the amount of drug in the polymer, the degradation rate (release rate of the drug), and the functionality of the drug need to be explored. Also, the molecular analysis of the drug and the polymer, and the electric field (fluid physics) effects on the solvent need to be investigated.

CHAPTER 7

CONCLUSION

Based in the data gathered, it is possible to obtain small diameter fibers by electrospinning using THF as a solvent. By combining the raw polymer, solvent, and drug in a simple mixing technique, the drug was able to reside in the polymer. This was evident when performing a DSC analysis and comparing the raw polymer to the electrospun fibers and the electrospun fibers with drug. Both the TGA analysis and DSC analysis, confirmed that the electrospinning process does not affect the polymer Tg or mass lost. The only characteristic that varied was in the morphology. The SEM analysis showed that the presence of the drug did not affect the diameter size of the fiber or the mass loss, but does affect the Tg.

Further analysis should be done to assess the amount of the drug present in the polymer, the functionality of the drug, shelf life of polymer drug delivery system, the release rate of the drug, and how to get the smaller fiber diameter. However diameter is dependent upon the problem, whether dealing with AVMs or tumors. If designing the system for tumors, the diameter should be under 8 microns, due to catheter diameter constraints. If the system's purpose is to plug up AVMs, then the diameter could be much larger, around 10-15 microns. The sample run for the electrospinning process involved the usage of MeCl, which provided fibers the day after mixing, whereas the THF did not. Testing out different solvents may help in making small diameter fibers within an allotted time constraint. Other solvents to look at would be chloroform and ethyl acetate, both dissolve BCNU and PLGA. A different drug may be used in place of BCNU (ex. tumor necrosis factor alpha, protein-tyrosine kinase inhibitors) and the effects

on the polymer characteristics investigated. Also, there was a variety of physical morphology that was observed, branching, rods, knobs, and pores that need set instructions on how to manipulate and guarantee a certain structure.

APPENDIX A

CHARACTERISTICS OF RESPECTIVE RATIOS OF PLA AND PLGA

Respective ratios contribute to mechanical toughness and strength found in either the crystalline or the semicrystalline form.

Polymer	Melting Pt (°C)	Glass Trans Temp (°C)	Modulus (Gpa)^a	Degrad Time (month)^b
PGA	225-230	35-40	7.0	6-12
LPLA	173-178	60-65	2.7	>24
DLPLA	Amorphous	55-60	1.9	12-16
PGA-TMC	N/A	N/A	2.4	6-12
85/15 DLPLG	Amorphous	50-55	2.0	5-6
75/25 DLPLG	Amorphous	50-55	2.0	4-5
65/35 DLPLG	Amorphous	45-50	2.0	3-4
50/50 DLPLG	Amorphous	45-50	2.0	1-2
a = tensile or flexural modulus				
b = time to complete mass loss.			Rate also depends on geometry	

[16]

APPENDIX B

BIOCOMPATIBILITY OF LACTIDE/GLYCOLIDE COPOLYMERS

Considerations on biocompatibility, the reaction of the patient to the material, and the effectiveness of the drug delivery system.

Lactide/Glycolide Copolymers: Review on Toxicity, Biocompatibility and Clinical Applications (data up to 1999)

1 Three cyclic monomers - glycolide, lactide, and ε-caprolactone

2 Biodegradation of the aliphatic polyesters occurs by bulk erosion. The polylactide/polyglycolide polymer chains are cleaved by hydrolysis to form monomeric acids and are eliminated from the body through the Krebs cycle, primarily as carbon dioxide and water in urine. Because the rate of hydrolysis of the polymer chain is dependent only on significant changes in temperature and pH or presence of catalyst, a very little difference is observed in rate of degradation at different body sites (Brandt et al. 1984, Cutright & Hunsuck 1971).

3 The role of enzymatic involvement in the biodegradation of the polylactide/polyglycolide polymer has been somewhat controversial. Most early literature conclude that bioerosion of these materials occurred strictly through hydrolysis with no enzymatic involvement (Puleo et al. 1998). Other investigators suggest that enzymes do ply a significant role in the breakdown of the breakdown of the lactgide/glycolide materials (Fukuzaki et al. 1990, Reed 1978, Williams 1977-

1981). Much of this speculation is based upon the differences observed between in vivo and in vitro degradation rates: it is supposed that a little enzyme involvement is expected in the early stages with polymers in the glassy state, whereas enzymes can play a significant role for polymers in the rubbery state (Holland et al. 1986).

4 Increased hydrophilia, a larger surface area, and a higher proportion of monomers promote biological degradation (Nakamura et al. 1989). The water uptake into the polymer is also influenced by the ratio of crystalline to amorphous regions: in general, amourphous regions are more easily affected by hydrolysis (Asano et al. 1989). The ratio of crystalline to amorphous regions in the polymer is dependent both on the physiological environment and on the stoichiometry of the monomers. In comparison to L-lactic acid, D-lactic acid increases, the extent of the amorphous regions (Engleberg & Kohn 1991, Wood 1980) and copolymers from lactic and glycolic acids are more easily degradable than their respective pure polymers (Craigt et al. 1975).

[19]

APPENDIX C

MECHANICAL PROPERTIES OF MEDISORB® POLYMERS

Summarized mechanical properties of polymer obtained from Alkermes.

Alkermes
Science that Delivers

MEDISORB®
BIOABSORBABLE POLYMERS

GENERAL MECHANICAL PROPERTIES

Polymers	5050 DL	100 DL	100 L (Custom)	9010 L/DL (Custom)
Formulation	50% poly d,l-lactide / 50% glycolide	100% poly d,l-lactide	100% poly l-lactide	90% poly-l-lactide / 10% d,l-lactide
Break stress, psi	8296	6108	7323	7614
% strain at break	5.2	5.0	5.5	5.2
Yield stress, psi	8371	6666	7678	8414
% strain at yield	5.1	3.7	4.9	4.5
Modulus, psi	189,340	207,617	182,762	210,680

MECHANICAL PROPERTIES OF POLY-L-LACTIDE / CAPROLACTONE COPOLYMERS

Polymer L-lactide/caprolactone Weight Ratio	50/50	75/25	85/15	90/10	95/5
Tensile Strength, psi					
At max.	80	1488	3254	6232	6900
At 100%	79	400	1822	None	None
At 300%	44	950	2615	None	None
Elongation, %					
To Yield	>1000	>400	>6.4	8.1	1.6
To Failure	>1000	>400	>500	8.1	1.6
Modulus, Kpsi	0.1	5.3	84	167	185
Shore D-hardness	5	52	87	91	95
Specific gravity	1.20	1.20	1.23	1.25	1.26
Compression molding temperature, °C	73 – 130	130 +/- 15	140 +/- 10	165 +/- 5	165 +/- 5

MECHANICAL PROPERTIES OF POLY-DL-LACTIDE / CAPROLACTONE COPOLYMERS

Polymer DL-lactide/caprolactone Weight Ratio	60/40	75/25	85/15	90/10	95/5
Tensile Strength, psi					
At max.	65	1300	1555	4453	5493
At 100%	65	224	1555	None	None
At 300%	43	332	1041	None	None
Elongation, %					
To Yield	-	-	-	5.6	-
To Failure	>400	>600	>500	5.6	7.2
Modulus, Kpsi	0.1	1.05	6.04	106	135
Shore D-hardness	0	42	79	88	95
Specific gravity	-	1.20	1.22	1.24	-
Compression molding temperature, °C	-	82 - 140	82 - 140	82 - 140	120

Customer Service
Tel 513-489-0294
Fax 513-489-7244

APPENDIX D

SOLUBILITY CHART OF MEDISORB® POLYMERS

Summarized solubility of polymer obtained from Alkermes.

Alkermes
Science that Delivers

MEDISORB®
BIOABSORBABLE POLYMERS

SOLUBILITY CHART

MEDISORB®	Ethyl acetate	Methylene chloride	Chloroform	Acetone	Dimethyl formamide (DMF)	Tetrahydro-furan (THF)	Hexafluoro-Isopropanol (HFIP)
100 L (Poly-L-Lactide)	ns	s	s	ns	ns	ns	s
100 DL	s	s	s	s	s	s	s
8515 DL	s	s	s	s	s	s	s
7525 DL	s	s	s	s	s	s	s
6535 DL	s	s	s	s	s	s	s
5050 DL	ss*	s	s	ss*	s	ss*	s
Caprolactone (PCL)	s	s	s	s	s	s	s
75:25 L-lactide/ PCL	s	s	s	s	s	s	s
80:20 DL-lactide/ PCL	s	s	s	s	s	s	s
100 PGA	ns	ns	ns	ns	ns	ns	s

ns = not soluble
ss * = slightly soluble (degree of solubility is dependent on molecular weight or IV)
s = soluble

Medisorb® is not soluble in water, ethanol, methanol, silicon oil , ethyl ether and petroleum ether (heptane, hexane etc.).

Customer Service
Tel 513-489-0294
Fax 513-489-7244

APPENDIX E

THERMAL ANALYSIS DATA OF MEDISORB® POLYMERS

Summarized thermal properties of polymer obtained from Alkermes.

MEDISORB® POLYMER Tg AND MELTING POINT DATA

Polymer	Formulation	Glass Transition Temp.°C	Melting Point °C
100 PGA	100 % polyglycolic acid	35 - 40	225 - 230
100 L	100 % poly-l-lactide	56 - 60	173 - 178
9010 G/L	90 % glycolide / 10 % l-lactide	35 - 45	180 - 200
100 DL	100 % d,l-lactide	50 - 55	Amorphous *
8515 DL	85% d,l-lactide / 15% glycolide	50 - 55	Amorphous *
7525 DL	75% d,l-lactide / 25% glycolide	48 - 53	Amorphous *
6535 DL	65% d,l-lactide / 35% glycolide	45 - 50	Amorphous *
5050 DL	50% d,l-lactide / 50% glycolide	43 - 48	Amorphous *
8515 DL/PCL	85% d,l-lactide / 15% polycaprolactone	20 - 25	Amorphous *
8515 L/PCL	85% l-lactide / 15% polycaprolactone	20 - 25	Amorphous *
7525 L/PCL	75% l-lactide / 25% polycaprolactone	13 - 20	Amorphous *
100 PCL	100% polycaprolactone	(-60) - (-65)	60

* Amorphous Polymers Process Temperature Range: 140 – 160 °C

Customer Service
Tel 513-489-0294
Fax 513-489-7244

APPENDIX F

CHEMICAL PROPERTIES OF BCNU

Summarized chemical properties of drug BCNU.

Poly(1,3-bis-p-carboxyphenoxypropane anhydride)

ABRAHAM J. DOMB AND ROBERT LANGER

ACRONYMS, TRADE NAMES BIODEL-CPP, Poly(CPP), Poly(CPP-SA)

CLASS Polyanhydrides

STRUCTURE BÿCOÿC $_6$H $_4$ ÿOÿCH $_2$ÿCH $_2$ ÿCH $_2$ÿOÿC $_6$H $_4$ÿCOOÿÜ

MAJOR APPLICATIONS Biodegradable polymer for controlled drug delivery in a form of implant or injectable microspheres (e.g., Gliadel ™ -BCNU-loaded wafer for the treatment of brain tumors).

PROPERTIES OF SPECIAL INTEREST Anhydride copolymers of 1,3-bis-p-carboxyphenoxypropane (CPP) with aliphatic diacids such as sebacic acid (SA) degrade in a physiological medium to CPP and SA. Matrices of the copolymers loaded with dissolved or dispersed drugs degrade in vitro and in vivo to constantly release the drugs for periods from 1±10 weeks.

PROPERTY	UNITS	CONDITIONS	VALUE	REFERENCE
Molecular weight		P(CPP-SA)		
	10^4 g mol $^{-1}$	GPC-polystyrene standards	M $_w$ 0 3±20, M $_n$ 0 0X5±3 Ð	
	dl g $^{-1}$	Viscosity 258C, dichloromethane	$_{sp}$ 0 0X2±0.9	Ð
IR (characteristic absorption frequencies)	cm $^{-1}$	Film on NaCl pellet	1,750, 1,810	(1)
		PSA	1,740, 1,770, 1,810	
		P(CPP-SA)	1,712, 1,773	
		P(CPP)		
Raman	cm $^{-1}$	Film on NaCl pellet		(1)
		PSA	1,739, 1,803	
		P(CPP-SA)	1,723, 1,765, 1,804	
		P(CPP)	1,712, 1,764	
UV (characteristic absorption wavelength)	nm	P(CPP-SA), dichloromethane	265	Ð
		CPP monomer, 1 N NaOH solution	265	
Optical rotation	Ð	Dichloromethane	No optical rotation	Ð

Poly(1,3-bis-p-carboxyphenoxypropane anhydride)

PROPERTY	UNITS	CONDITIONS	VALUE				REFERENCE
Solubility	mg ml $^{-1}$		P(CPP-SA), 0±60 mol% CPP		P(CPP-SA), 70± 100 mol% CPP		(2)
		Chloroform	b300		`1		
		Dichloromethane	b300		`1		
		Tetrahydrofuran	20		`1		
		Ketones	1		`1		
		Ethyl acetate	`1		`1		
		Alkanes and arenes	`1		`1		
		Ethers	`1		`1		
		Water	`1		`1		
Mark±Houwink parameters: K and a ml g	$^{-1}$ None	$CHCl_3$, 238C	K ß 3X88 a ß 0X658				(3)
Thermal properties		P(CPP-A), DSC, 108C min $^{-1}$	0:100 22:78 46:54 100:0 (3)				
	K	T_m	359.0	339.0	458.0	513.0	
	K	T_g	333.1	320.0	274.8	369.0	
	kJ kg $^{-1}$	ÁH	150.7	64.0	13.0	110.9	
Crystallinity	%	P(CPP-SA), powder, X-ray diffraction	0:100 22:78 46:54 100:0 (3)				
		X_c	Ð	30.0	6.1	Ð	
		W_c	66.0	35.0	14.2	61.4	
Comonomer sequence distribution		P(CPP-SA), ^{1}H-NMR, $CDCl_3$	8:92	22:78 59:41 49:51 (3)			
		Probability for SA-SA	0.86	0.61	0.36	0.24	
		Probability for SA-CPP	0.14	0.34	0.47	0.49	
		Average block length L(SA) 12.3		4.6	2.5	2.0	
		Degree of randomness	0.3	0.7	0.9	1.0	
Stability in chloroform solution (decrease in M_w) (anhydride interchange depolymerization)			P(CPP-SA) 0:100	20:80	40:50		(4)
Depolymerization rate constant	t^{-1}	378C	0.1325	0.1535	0.0743		
Activation energy	kcal mol $^{-1}$	K^{-1}	8.08	8.27	7.27		
Erosion rate	mg h $^{-1}$	P(CPP-SA), 14 Å 1X2 mm disc, 0.1 M phosphate buffer, pH 7.4, 378C	0:100 22:78 49:51 100:0				(5)
		SA	2.3	1.8	0.4	Ð	
		CPP	Ð	0.5	0.3	`0.01	

Page

Poly(1,3-bis-p-carboxyphenoxypropane anhydride)

PROPERTY	UNITS	CONDITIONS	VALUE		REFERENCE
Erosion front	mm day $^{-1}$	0.1 M phosphate buffer, pH 7.4, 378C			(6)
		P(CPP-SA), 20:80	106 Æ 5		
		P(CPP-SA), 50:50	118 Æ 18		
Elimination in vivo	%		CPP	SA	(7)
		7 days in rat brain	2	95	
		21 days in rat brain	64	100	
Drug release in vitro % day	$^{-1}$	P(CPP-SA), 20:80			(7)
		3.8% BCNU in disc	30		(6)
		5% indomethacin in disc	9		
Drug release in vivo % day	$^{-1}$	3.8% BCNU disc implanted in rat brain	16		(7)
Biocompatibility	Compatible with human brain				(8)
	Compatible with rabbit brain, cornea, muscle, subcutane				
Supplier	Guilford Pharmaceuticals, Inc., Baltimore, Maryland, USA				

REFERENCES

1. Tudor, A. M., et al. Spectrochimica Acta 9/10 (1991): 1,335±1,343.
2. Domb, A. J., and M. Maniar. J. Polym. Sci. 31 (1993): 1,275±1,285.
3. Ron, E., et al. Macromolecules 24 (1991): 2,278±2,282.
4. Domb, A. J., and R. Langer. Macromolecules 22 (1989): 2,117±2,122.
5. Tamada, J. A., and R. Langer. Proc. Natl. Acad. Sci. USA 90 (1993): 552.
6. Gopferich, A., D. Karydas, and R. Langer. Eur. J. Pharm. Biopharm. 41 (1995): 81±87.
7. Domb, A. J., et al. Biomaterials 15 (1994): 681±688.
8. Domb, A. J., S. Amselem, R. Langer, and M. Maniar. In Designed to Degrade Biomedical Polymers, edited by S. Shalaby. Carl Hauser Verlag, 1994, pp. 69±96.

APPENDIX G

GMP ANALYSIS OF 75/25 DLPLGA POLYMER

Finished product specification of Medisorb® polymer 75/25 DLPLGA.

Alkermes

Certificate of Analysis

Medisorb® 7525 DL High IV
Finished Product Specification 1751001

Lot #: 0180-452
Date of Manufacture: 06/28/00

Test	Specification	Result
Inherent Viscosity	0.66 – 0.80 dL/g	0.76 dL/g
Residual Monomer	2.0% Total Maximum	1.6%
% d, l-lactide	Report Result	1.5 %
% glycolide	Report Result	0.05%
Copolymer Mole Ratio		
d, l-lactide	70 – 80 mole %	75 mole %
glycolide	20 – 30 mole %	25 mole %
Heavy Metals	10 ppm, Total, Maximum	<10 ppm
Glass transition temperature	Report Tg	49.80° C
Molecular Weight, Mw	Report Result	113 Kd
Mn	Report Result	69 Kd
Polydispersity	Report Result	1.649

The tests and associated criteria specified in this Certificate of Analysis conform with the Finished Product Specifications established by Alkermes Controlled Therapeutics II.

The manufacturing, quality control and environmental records associated with the above referenced lot of Medisorb® 7525 DL High IV have been reviewed and found to be complete. The Quality Control testing of the lot complies with the Finished Product Specification #1751001 established by Alkermes Controlled Therapeutics II. The batch was produced in compliance with current Good Manufacturing Practices as they apply to the production of finished material for distribution. This lot of material is released for distribution.

Quality Assurance _____ Date: 8-9-00
Melissa A. Griffith, Quality Assurance Associate

APPENDIX H

GMP ANALYSIS OF 85/15 DLPLGA POLYMER

Finished product specification of Medisorb® polymer 85/15 DLPLGA.

Alkermes

Certificate of Analysis
Medisorb® 8515 DL High IV
FPS 1851001

Lot #: W3059-602

Date of Manufacture: 02-28-03

Test	Specification	Result
Inherent Viscosity	0.66 – 0.80 dL/g	0.76 dL/g
Residual Monomers	2.0 % total maximum	1.8 %
d, l-lactide	Report d, l-lactide	1.7 %
glycolide	Report glycolide	0.05 %
Copolymer d, l-lactide	80 – 90 mole %	85 %
Copolymer glycolide	10 – 20 mole %	15 %
Heavy Metals	10 ppm, total maximum	< 10 ppm
Glass Transition Temperature	Report Tg	50.8 ° C
Molecular Weight	Report Mw	123.6 kD
	Report Mn	80.4 kD
	Report Polydispersity	1.54

The manufacturing, quality control and environmental records associated with the above referenced lot of Medisorb® 8515-DL High IV have been reviewed and found to be complete. The Quality Control testing of the lot complies with the Finished Product Specification 1851001 established by Alkermes Controlled Therapeutics II. The batch was produced in compliance with current Good Manufacturing Practices a they apply to the production of finished material for distribution. This lot of material is released for distribution.

Prepared by_____ Date: 3-27-03
Kathy Miller
Quality Assurance Associate

Reviewed by_____ Date 03-27-2003
Melissa Maple
Quality Assurance Associate

Lot #: W3059-602 Page 1 of 1

APPENDIX I

NON-GMP ANALYSIS OF 80/20 DLPLGA POLYMER

Finished product specification of Medisorb® polymer 80/20 DLPLGA.

Alkermes

ANALYTICAL REPORT

Experimental Medisorb® 8020 DL High IV
Batch No. 00-141-87
Date of Manufacture: 05/29/01

Description	**Result**
Inherent Viscosity	0.62 dL/g

Reviewed by : _____ Date : 6/15/01

APPENDIX J

POLYMER CHARACTERISTICS OF MEDISORB® POLYMERS

Summarized characteristics of DL polymers.

Medisorb POLYMERS	INHERENT VISCOSITY(DL/G)	DL LACTIDE/ GLYCOLIDE MOLE RATIO	DEGRADATION INFORMATION
100 DL HIGH IV	0.66 - 0.80	100 / 0	12 - 16 months
100 DL LOW IV	0.50 - 0.65		
8515 DL HIGH IV	0.66 - 0.80	85 / 15	5 - 6 months
8515 DL LOW IV	0.50 - 0.65		
7525 DL HIGH IV	0.66 - 0.80	75 / 25	4 - 5 months
7525 DL LOW IV	0.50 - 0.65		
6535 DL HIGH IV	0.66 - 0.80	65 / 35	3 - 4 months
6535 DL LOW IV	0.50 - 0.65		
5050 DL HIGH IV	0.66 - 0.80	50 / 50	1 - 2 months
5050 DL LOW IV	0.50 - 0.65		
5050 DL 1A	0.08 - 0.12	50 / 50	1 - 2 weeks
5050 DL 2A	0.13 - 0.20		2 - 3 weeks
5050 DL 2.5A	0.21 - 0.31		2 - 4 weeks
5050 DL 3A	0.25 - 0.43		3 - 4 weeks
5050 DL 4A	0.38 - 0.48		3 - 4 weeks

APPENDIX K

ENVIRONMENTALLY SENSITIVE DRUG RELEASE SYSTEMS

Summarized description of environmentally sensitive drug release systems.

Stimulus	Hydrogel	Mechanism
pH	Acidic or basic hydrogel	Change in pH — swelling — release of drug
Ionic strength	Ionic hydrogel	Change in ionic strength — change in concentration of ions inside gel — change in swelling — release of drug
Chemical species	Hydrogel containing electron-accepting groups	Electron-donating compounds — formation of charge/transfer complex — change in swelling — release of drug
Enzyme-substrate	Hydrogel containing immobilized enzymes	Substrate present — enzymatic conversion — product changes swelling of gel — release of drug
Magnetic	Magnetic particles dispersed in alginate microshperes	Applied magnetic field — change in pores in gel — change in swelling — release of drug
Thermal	Thermoresponsive hrydrogel poly(N-isopro-pylacrylamide)	Change in temperature — change in polymer-polymer and water-polymer interactions — change in swelling — release of drug
Electrical	Polyelectrolyte hydrogel	Applied electric field — membrane charging — electrophoresis of charged drug — change in swelling — release of drug
Ultrasound irradiation	Ethylene-vinyl alcohol hydrogel	Ultrasound irradiation — temperature increase — release of drug

REFERENCES

1. "Electrospinning," *Department of Chemical Engineering, Virginia Tech.*, 2001.

2. Y.M. Shin, M.M. Hohman, M.P. Brenner, G.C. Rutledge, "Electrospinning: A whipping fluid jet generates submicron polymer fibers," *Applied Physics Letters*, vol. 78, number 8, February 2001.

3. M.M. Hohman, M. Shin, G. Rutledge, M. P. Brenner, "Electrospinning and electrically forced jets. II. Applications," *Physics of Fluids*, vol. 13, number 8, August 2001.

4. C. J. Buchko, L.C. Chen, Y. Shen, D.C. Martin, "Processing and microstructural characterization of porous biocompatible protein polymer thin films," *Elsevier Polymer*, 40, pp. 7397-7407, 1999.

5. "Modeling Reveals Secrets of Electrospinning," *MPC Industry Collegium Report*, vol. 17, No. 3, June 2001.

6. "Arterio Venous Malformations of the Brain and Spine," *The Cerebrovascular Center of the Neurological Institute, Columbia University*, 1995.

7. "Locating AVMs," *Computer Graphics Group, Brown University.*

8. Dr. A. Vincent Thamburaj, "Cerebral AVMs," *Neurosurgery, Apollo Hospitals*, Chennai, India.

9. A primer on brain tumors, *Brain Tumor Foundation*, New York City. http://www.braintumorfoundation.org/

10. P. I. Musey, S. M. Ibim, and N. K. Talukder, "Development of Artificial Blood Vessels: Seeding and Proliferation Characteristics of Endothelial and Smooth Muscle Cells on Biodegradable Membranes," *Ann. N.Y. Acad. Sci.* 961: pp. 279-283, (2002). © 2002 New York Academy of Sciences.

11. E. J. Topol, MD; P. W. Serruys, MD, PhD, "Frontiers in Interventional Cardiology (Clinical Cardiology: New Frontiers)," © 1998 American Heart Association, Inc., October 1998.

12. J. R. Fuchs, MD, B. A. Nasseri, MD, and J. P. Vacanti, MD, "Tissue Engineering: A 21st Century Solution to Surgical Reconstruction," *Elsevier Science Inc.* © 2001 by The Society of Thoracic Surgeons.

13. J. Katz, "Developments in Medical Polymers for Biomaterials Applications As materials designers confront the fundamental challenges of medical science, the discovery of new biocompatible polymers is creating unprecedented excitement," January 2001.

14. J. Robinson, P. M. Saint Louis, A. Padmaraju, "Polymer in Medicine CE 435 Introduction to Polymers," *Department of Chemical Engineering, University at Buffalo-SUNY*, April 2001.

15. W.B. Gleason, "Bioabsorbable Polymers," *Department of Biomedical Engineering, University of Minnesotta*, 1998.

16. J.C. Middleton, A.J. Tipton, "Synthetic Biodegradable Polymers as Medical Devices," *MPB archive*, March 1998.

17. J. A. Field, "Dissolvable Sutures: How Do Sutures Dissolve?," *University of Pennsilvania.*

18. "Polymeric Drug Delivery - A Review," *Drugdel.com,* 2000.

19. "Medisorb® Polymer Products", Alkermes, Inc., 2003.

20. L. Brannon-Peppas, "Polymers in Controlled Drug Delivery," November 1997.

21. D. Acquafredda, "BCNU For Brain Tumors," *The Musella Foundation*, 1993-2003.

22. Guilford Pharmaceuticals, "Gliadel® Wafer," *Physician's Desk Reference*, pp 1723-1725, Copyright © 2002.

23. A.I. Torres-Suarez, V. Ruz, M. E. Gil-Alegre, J. A. Bernabeu, M. A. Camacho, "Characterization of biodegradable BCNU-loaded microspheres prepared by the solvent evaporation-extraction method," *SciFinder* ®, 2003.

24. WJ. Li, C. T. Laurencin, E. J. Caterson, R. S. Tuan, F. K. Ko, "Electrospun nanaofibers structure: a novel scaffold for tissue engineering," *Journal of Biomedical Materials Research*, vol. 60, Issue 4, pp. 613-621, 2002.